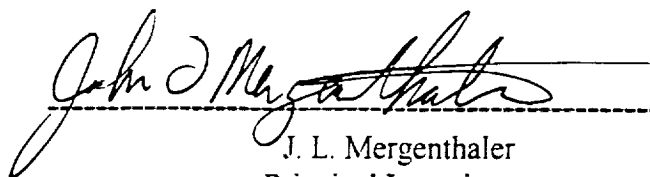


Final Report for NASA Contract NAS5-98044

Cirrus and Polar Stratospheric Cloud Studies using CLAES Data

Prepared for:
NASA/Goddard Space Flight Center, Earth Sciences Procurement Office
Greenbelt, Maryland



J. L. Mergenthaler
Principal Investigator

Lockheed Martin Advanced Technology Center
Lockheed Martin Missiles and Space
Palo Alto, CA 94304-1187

Introduction:

We've concluded a 3 year (Period of Performance- January 21, 1998 to February 28, 2001) Study of cirrus and polar stratospheric clouds using CLAES data. We have described the progress of this study in monthly reports, UARS science team meetings, American Geophysical Society Meeting, refereed publications and collaborative publications.

Statement of Work:

1. Establish CLAES cloud detection criteria, refine techniques of PSC and cirrus cloud-top temperature retrieval from CLAES data and examine ways of representing the diurnal cycle of cloudiness in the tropics.
2. Complete a case study using data from the Tropical Ocean Global Atmosphere Coupled Ocean-Atmosphere Response Experiment (TOGA COARE) field campaigns during a CLAES overpass
3. Compare cloud occurrence statistics derived from CLAES with data from the International Satellite Cloud Climatology Project (ISCCP), High Resolution Infrared Sounder (HIRS) and Stratospheric Aerosol and Gas Experiment II; construct a cloud dataset on a week by week basis and make all results available in numerical form.
4. Provide results from these studies to a wider community through papers in the refereed literature and presentations at scientific meetings.

The remainder of the report will describe our progress in each of the four areas.

I. Establish CLAES cloud detection criteria, refine techniques of PSC and cirrus cloud-top temperature retrieval from CLAES data and examine ways of representing the diurnal cycle of cloudiness in the tropics.

Ice clouds are of course just a special type of aerosol. CLAES is a very sensitive detector of aerosol capable of detecting aerosol with volume absorption coefficients, k_{abs} , down to about $1.0\text{E-}06/\text{km}$. Since UARS launched in October, 1991, the entire CLAES mission was performed under extremely high stratospheric aerosol loading resulting from the June 15, 1991

eruption of Mt. Pinatubo.

The aerosol from Mount Pinatubo was mainly confined to the lower stratosphere well above tropical cirrus which is confined below the tropopause. Also the maximum k_{abs} for stratospheric aerosol measured by CLAES in our preferred 12.8 μm channel is about 10^{-3} km^{-1} where as much higher values can be observed in areas likely to have polar stratospheric cloud (PSC) or cirrus. The background stratospheric aerosol was also declining continually during the CLAES mission where as cirrus proceeds through a annual cycle with some deviation due to ENSO phenomena. Using our past experience at discriminating PSCs with a threshold approach [Mergenthaler *et al.*, 1997], we established $k_{\text{abs}} = 9.0\text{E-}04/\text{km}$ as a threshold for near-tropopause cirrus. This threshold produces cirrus distributions which compare favorably with the near-tropopause tropical cirrus distributions in the Wang *et al.* (1996) cirrus climatology compiled from five years worth of SAGE II data. At higher levels in the tropics above about 14.5 km the vast majority of SAGE II observations involve subvisual cirrus. The good agreement between CLAES cirrus observations and SAGE II observations indicate CLAES too, detects the majority of subvisual cirrus. A detailed description of the establishment of the cloud detection threshold and comparison with the SAGE II climatology is included as Appendix A, a reprint of Mergenthaler *et al.*, 1999, *Cryogenic Limb Etalon Array Spectrometer Observations of Tropical Cirrus*.

We studied remotely sensing the temperature of cirrus using the limb radiance measured by CLAES in the 12.8 μm channel. We examined a case where the limb brightness temperature observed by CLAES greatly exceeded the ambient temperature determined from NCEP and local radiosondes. This was part of our TOGA COARE case study. Figure 1 shows the cloud top temperatures at 12 UTC from the ISCCP analysis of GMS-4 IR/VIS data on January 19, 1993. The CLAES "3at" aerosol data at 100 hPa are over plotted with their observation time. The symbols are filled according to the aerosol emissivity, $\epsilon = 1 - \exp(-k_{\text{abs}} * 400)$, where 400 km is the CLAES LOS path through a 2.5 km thick shell in the limb view. If the symbol is filled CLAES has detected a cloud. Near Yap, CLAES detects clouds where no cold cloud tops are observed. Figure 2 shows that local radiosonde temperatures from Yap and Koror are about 10 degrees less than the limb brightness temperatures observed by CLAES. In order to explain this discrepancy in temperatures we modeled the radiative transfer of the thin cirrus with a

simple Monte Carlo model. Our results, show that the limb brightness can be greatly enhanced as high radiance from the warm surface and lower atmosphere are scattered into the limb by thin cirrus. The amount of scattering is related to particle size and cloud thickness. If the particles have radii below two micrometers they are not effective at scattering the $12.8\ \mu\text{m}$ radiation observed by CLAES, bigger particles can enhance the limb brightness enough to match the observations. As the cloud thickens, radiation upwelling from the surface is absorbed in the cloud and not scattered so the limb brightness temperature seeks the ambient temperature. Thus the limb brightness measurement becomes akin to cloud top temperature measurements by operational nadir viewing instruments which routinely report cloud top temperatures.

Our conclusions about cloud brightness temperatures is that: 1.) The brightness temperature of near-tropopause clouds is not a good indicator of their ambient temperature due to scatter effects. 2.) Cirrus-related limb brightness temperatures that exceed the ambient temperature by several degrees evidently reveal thin cirrus that are exposed to high surface temperatures. These clouds are more important from a radiative standpoint than cirrus that overlay cold cloud tops. The CLAES data is a unique source of this information until new instruments like HRDLS are in place

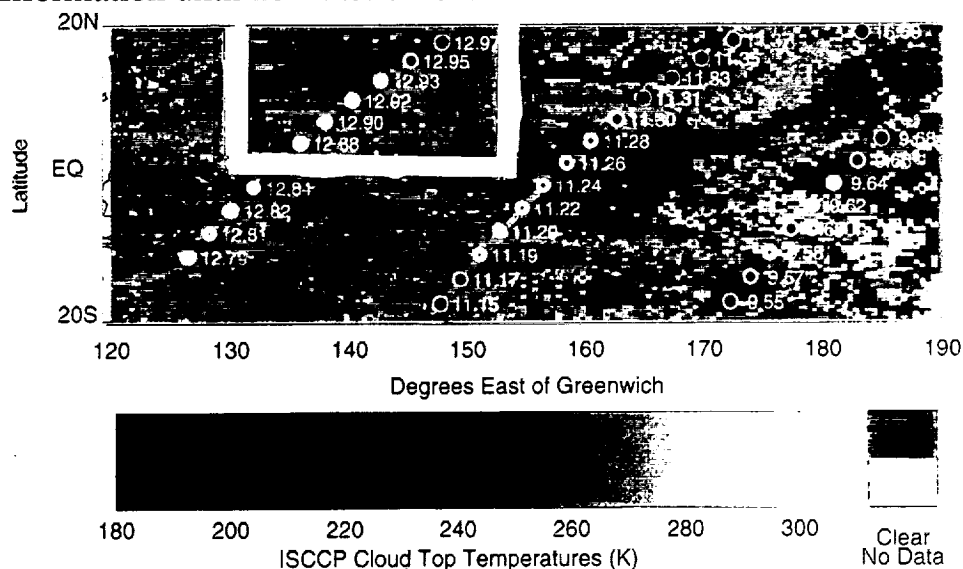


Figure 1. CLAES 100 hPa cloud measurements superposed on the ISCCP 12 UTC cloud top temperatures for January 19, 1993. The white box shows the area near Yap where CLAES detects clouds, and high limb brightness temperatures.

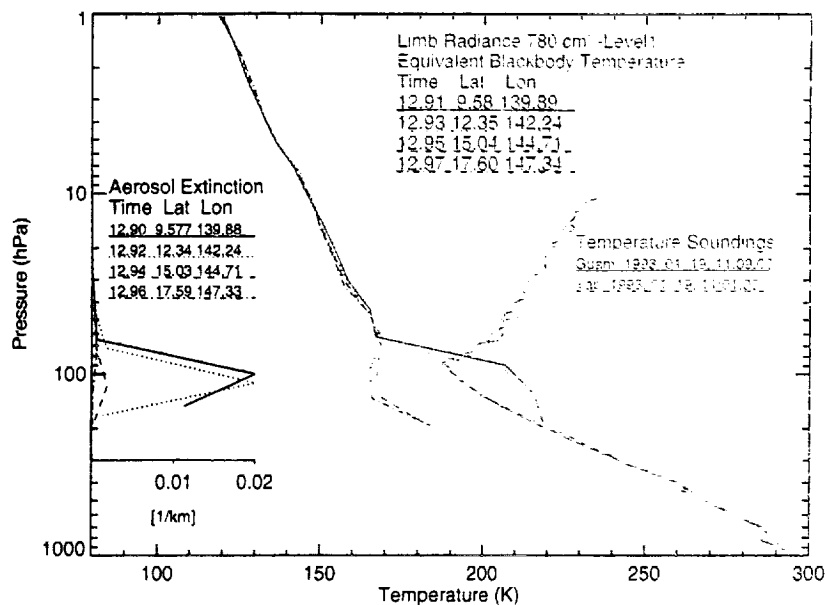


Figure 2. The Limb brightness observed by CLAES and the local radiosonde temperature profile near Yap near 12 UTC at Yap January 19, 1993. The retrieved aerosol volume absorption coefficients are also shown.

$k_{ext}(12.8 \mu m)$ [km ⁻¹]	Particle Radius [μm], ω_0 , g				
	20.0, 0.50, 0.91	5.0, 0.43, 0.77	2.0, 0.24, 0.30	1.0, 0.06, 0.07	0.8, 0.04, 0.04
0.001	177	180	175	168	166
0.01	211	216	206	195	192
0.1	208	213	205	195	193
1.0	198	202	198	193	191

Table 1. The calculated limb brightness temperature of a 2.5 km thick cylindrical cloud of radius 200 km centered at 16 km altitude. Temperatures are shown for various cloud aerosol volume absorption coefficient and mean particle size. Particle single scattering albedo and asymmetry factor are also shown.

The emission measuring instruments (CLAES, ISAMS, and MLS) were intended to provide measurements through the diurnal cycle. We constructed diurnal cycle representations for tropical cirrus by binning cloud occurrence data in hourly or 4 hourly local solar time bins. One of the peculiarities of CLAES's sampling that CLAES didn't sample near-noon in the tropics to prevent depletion of cryogen due to getting sunlight on the telescope baffles. This results in a spatially and temporally nonuniform sampling pattern in the tropics. Nevertheless we constructed the diurnal cycle from each season of CLAES data availability. Figure 3 is an example of such a construction where the 146 hPa data from summer 1992 (JJA 92) in the region from 22S to 22N has been used. We added error bars based on the standard deviation of the mean. There are fewer measurements near-noon so the error bars are relatively large, but through the rest of the cycle the sampling is more uniform and so are the error bars. We found it useful to use only areas where the mean (over time) cloud frequency of occurrence was at least some minimum (in this example) 0.1, this prevents the cycle containing cloud free areas that have no diurnal variation.

The diurnal cycle shown in Figure 3 is represented peak cloudiness near sunset and sunrise and a minimum near midnight. The midnight minimum are about 20% less than the maxima. The near-midnight minimum is a characteristic of all seasons. Our conclusion to this segment of work is that 1) a coherent diurnal cycle of upper tropospheric cirrus can be formed from CLAES cirrus data 2.) the interpretation of the near-noon data is complicated by sampling considerations 3.) these are publishable first-of-a-kind results because they include subvisual cirrus that is largely invisible to nadir viewing instruments but comparisons with other sources of cloud diurnal behavior and interpretation remain.

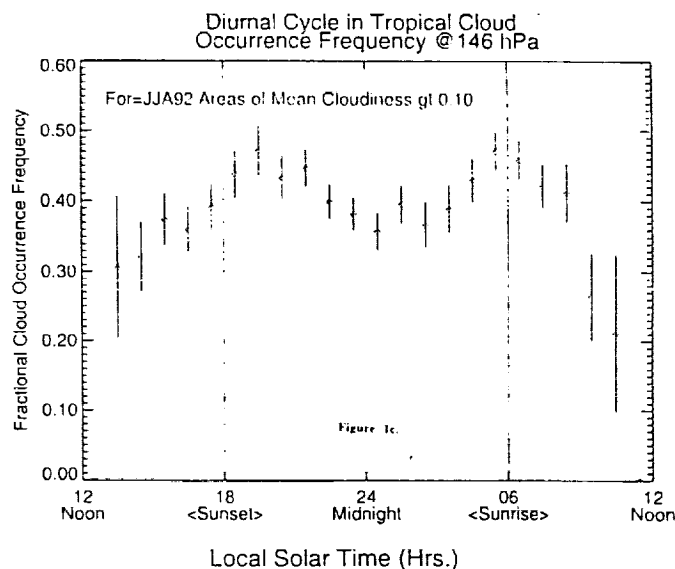


Figure 3. The diurnal cycle of cirrus at 146 hPa constructed from CLAES data in the region 22S to 22N for June, July and August, 1992. (JJA92)

2. Complete a case study using data from the Tropical Ocean Global Atmosphere Coupled Ocean-Atmosphere Response Experiment (TOGA COARE) field campaigns during a CLAES overpass

In addition to using TOGA COARE data for the limb brightness study discussed above, we have used nearly-coincident DC8 lidar data and ISCCP data to compare the CLAES cirrus observations on a scale smaller than the global and seasonal comparisons with the SAGE II climatology. In addition to these comparisons we used weekly cloud frequency of occurrence statistics to track the progress of convection organized by the Madden Julian oscillation in the TOGA COARE region. The observation of the Madden-Julian oscillation, the most important intraseasonal event effecting tropical weather, is a first for a limb sounding instrument. Solar occultation instrument that shares the sensitivity of CLAES for observing subvisual cirrus are not practical for tracking this rather small scale event. SAGE II for example typically gathers fewer than 4 profiles in the tropics (20N-20S) whereas CLAES obtains 280.

A major goal of the TOGA COARE campaign was to understand the interaction between the atmosphere and ocean to sustain the "warm pool" in

the western Pacific. The CLAES observations supplement the data set with occurrence statistics for subvisual clouds throughout the study period. The study is discussed in some detail in Appendix B, a manuscript that will be resubmitted to the *Journal of Geophysical Research* since the addition of the Madden Julian results.

3. Compare cloud occurrence statistics derived from CLAES with data from the International Satellite Cloud Climatology Project (ISCCP), High Resolution Infrared Sounder (HIRS) and Stratospheric Aerosol and Gas Experiment II; construct a cloud dataset on a week by week basis and make all results available in numerical form.

As discussed above and in Appendix A, [Mergenthaler *et al.*, 1999] we have successfully compared CLAES cloud frequency of occurrence with the 5-year climatology compiled from SAGE II observations by Wang *et al.* (1996). According to Wang *et al.* (1996) the predominance of near-tropopause cirrus observations by SAGE II involve subvisual cirrus. In Appendix B we compare nearly coincident DC8 lidar measurements, ISCCP cloud top analysis and CLAES cirrus measurements. We've done similar comparisons not shown in Appendix B. We conclude from these studies and others (e.g. Jin *et al.*, 1996) that ISCCP analysis is largely insensitive to the thin clouds seen by SAGE II and CLAES. HIRS is also insensitive to the subvisual cirrus seen by SAGE II (Wylie and Wang, 1997).

We've posted a readme.txt, an idl.sav file, and a reading plotting program to retrieve and, to some extent display, week cloud frequency of occurrence statistics for the CLAES mission on 10 degree longitude by 5 degree longitude bins for the 215, 146, 100, 68 and 46 hPa levels. The data is posted on anonymous ftp at claes.spasci.com in the [anonymous.clouds] directory.

4. Provide results from these studies to a wider community through papers in the refereed literature and presentations at scientific meetings.

The results from this contract have widely disseminated and in a timely fashion so that they can be used by others. We have presented contract related papers at American Geophysical Union Meetings.

Conference Presentations:

1. Spring 1998 AGU, J. L. Mergenthaler et. al., Variability in tropical cirrus as observed by UARS-CLAES
2. Spring 1999 AGU, J. L. Mergenthaler et. al. Comparison of CLAES and GMS-4 measurements
3. Spring 2000 AGU, J. L. Mergenthaler et. al. Observations of the diurnal cycle of near-tropopause tropical cirrus

Publications:

Mergenthaler, J. L., A. E. Roche, J. B. Kumer, and G.A. Ely, "Cryogenic limb etalon array spectrometer observations of tropical cirrus", *J. Geophys. Res.*, 104, 22,183-22,194, 1999.

Publications (cont.):

We collaborated on the following publications that use our cirrus and PSC results:

Sandor, B. J., E. J. Jensen, E. M. Stone, W. G. Read, J. W. Waters, and J. L. Mergenthaler, "Upper tropospheric humidity and thin cirrus", *Geophys. Res. Lett.*, 27, 2645-2648, 2000.

Jensen, E. J., W. G. Read, J. Mergenthaler, B.J. Sandor, L. Pfister, and A. Tabazadeh, "High humidities and subvisible cirrus near the tropical tropopause ", *Geophys. Res. Lett.*, 26, 2645-2648, 1999.

Tabazadeh A., M. L. Santee, H. Pumphrey, M. Y. Danilin, P. Hamill, J. L. Mergenthaler et al., "Quantifying denitrification and its effect on ozone recovery", *Science*, 288, 1407, 2000.

Danilin, M.Y., M. L. Santee, J. M. Rodriguez, M. E. W. Ko, J. L. Mergenthaler, J. B. Kumer, A. Tabazadeh and N. J. Livesey Trajectory hunting: A case study of rapid chlorine activation December 1992 as seen by UARS. *J. Geophys. Res.*, 105, 4003-4018, 2000.

Danilin, M.Y., J. M. Rodriguez, W. Hu, M. E. W. Ko, D. K. Weisenstein, J. B. Kumer, J. L. Mergenthaler, J. M. Russell III, M. Koike, G. K. Yue, N. B. Jones, and P. V. Johnston, "Nitrogen species in the Post Pinatubo atmosphere: Model Analysis utilizing UARS Measurements," *J. Geophys. Res.*, 104, 8247-8267, 1999.

These manuscripts are being revised.

Read, W. G., J. W. waters , D. L. Wu, E. M. Stone, Z. Shippony, A. C. Smedley, C. C. SmallComb, S. Oltmans, D. Kley, H. G. J. Smit, J. L. Mergenthaler and M. K. Karki, UARS MLS upper tropospheric humidity: measurement, method an validation, (in revision *for J. Geophys Res*).

Stone, E.M., A. Tabazadeh, E. Jensen, H. C. Pumphrey, M. Santee, and J. L. Mergenthaler, The onset, extent and duration of dehydration in the southern hemisphere polar vortex, (in revision *for J. Geophys Res*).

Publications (cont.):

We're resubmitting to the Journal of Geophysical Research the manuscript, Appendix B,

Mergenthaler et al., Observations of near-tropopause cirrus: A case study combining UARS and TOGA COARE data.

We assisted (Dr. Jochin Horn) in the SOFIA operations with cirrus data. as acknowledged in Horn, J. M. N. and Becklin, E. E., "Optimized Flight Planning for SOFIA", Proceedings of the Society of Photo Optical Instrumentation Engineers (SPIE), 4014, 2000.

References:

- Jin, Y., W. B. Rossow, and D. P. Wylie, Comparison of the climatologies of high-level clouds from HIRS and ISCCP, *J. Clim.*, 9, 2,850-2,879, 1996.
- Mergenthaler, J. L., A. E. Roche, J. B. Kumer, and G. A. Ely, Cryogenic Limb Etalon Array observations of tropical cirrus, *J. Geophys. Res.*, 104, 22,183-22,194, 1999.
- Mergenthaler, J. L., A. E. Roche, J. B. Kumer, and G. A. Ely, Cryogenic Limb Etalon Array observations of tropical cirrus, *J. Geophys. Res.*, 104, 22,183-22,194, 1999.
- Wang, P. -H., P. Minnis, M. O. McCormick, G. S. Kent, G. K. Yue, and K.M. Skeens, A 6-year climatology of cloud occurrence frequency from Stratospheric Aerosol and Gas Experiment II observations (1985-1990), *J. Geophys. Res.*, 101, 22,407- 29,429, 1996.
- Wylie, D. P., and P. -H. Wang, Comparison of cloud frequency data from the high-resolution infrared radiometer sounder and the Stratospheric Aerosol and Gas Experiment II, *J. Geophys. Res.*, 102, 29,893-29,900, 1997.

Cryogenic Limb Array Etalon Spectrometer observations of tropical cirrus

J. L. Mergenthaler, A. E. Roche, J. B. Kumer, and G. A. Ely

Lockheed Martin Advanced Technology Center, Palo Alto, California

Abstract. The seasonal evolution and spatial distribution of upper tropospheric tropical cirrus have been analyzed using a 19-month record of infrared aerosol volume absorption coefficients obtained by the Cryogenic Limb Array Etalon Spectrometer (CLAES) aboard the Upper Atmosphere Research Satellite (UARS). An empirical method of separating clouds from background volcanic aerosol is described. Cloud occurrence frequencies are compared with the Stratospheric Aerosol and Gas Experiment (SAGE) II cloud climatology of Wang *et al.* [1996]. The seasonal distribution of clouds derived from CLAES agrees well with the SAGE II results that show predominantly subvisual cirrus in this region. This agreement demonstrates that CLAES data contain information describing subvisual cirrus in addition to thicker clouds. Examples of interannual variations in cloud occurrence frequency observable in the CLAES data are discussed. The eastward shift in cloud occurrence frequency over the western Pacific accompanying the 1992 El Niño was observed. Substantially fewer cirrus were seen at the 68-hPa level in the winter of 1991–1992 compared with 1992–1993. This variation could be related to either El Niño or reduced convection during a period when Mount Pinatubo stratospheric aerosol cooled the tropics.

1. Introduction

Interest in tropical cirrus clouds stems from their radiative effects [Ramanathan and Collins, 1991], their links to stratospheric hydration and dehydration [Danielsen, 1993; Jensen *et al.*, 1996; Rosenfield *et al.*, 1998], and their role in heterogeneous chemical reactions in the upper troposphere [Solomon *et al.*, 1997]. The most complete data set describing the seasonal variability and geographical distribution of high-altitude tropical cirrus has come from the limb-viewing occultation observations of the Stratospheric Aerosol and Gas Experiment (SAGE) II [Wang *et al.*, 1996]. These data show that the most frequently occurring cirrus are sufficiently tenuous to be invisible to ground observers and the nadir-viewing satellite-borne instruments that gather operational meteorological data. For this reason, data sets describing these thin cirrus are very limited.

While the SAGE II data provide a good climatological description of thin cirrus, aerosol data from the Cryogenic Limb Array Etalon Spectrometer (CLAES) instrument on the Upper Atmosphere Research Satellite (UARS) [Roche *et al.*, 1993] obtained in thermal emission provide an opportunity to observe thin cirrus with much more frequent, near-global sampling. Although CLAES was designed to observe the stratosphere, the lower-altitude limit of its observations was frequently below the tropopause, particularly in the tropics, where the tropopause is high. For example, CLAES typically gathered about 280 profile measurements per day within 20° of the equator, while SAGE II averages fewer than four. This increased data density eliminates the need to average over several years to examine the seasonal behavior of near-

tropopause clouds and provides a more detailed look at their interannual variations.

CLAES operated from October 1991 to May 1993. During this period, volcanic aerosol loading from the Mount Pinatubo eruption (June 15, 1991) reached its maximum, and a moderately strong El Niño developed in the winter of 1991–1992. Analysis of the CLAES data provides an opportunity to investigate changes in cloud occurrence associated with these phenomena.

In addition to its value as a stand-alone data set, the CLAES data complement other data sets and improve our ability to obtain a more complete description of the atmosphere. For example, CLAES data are concurrent with intensive operation periods of the Tropical Ocean–Global Atmosphere Coupled Ocean–Atmosphere Response Experiment (TOGA COARE) [Webster and Lukas, 1992] and the Central Equatorial Pacific Experiment (CEPEX). In addition, CLAES was coaligned with the Microwave Limb Sounder (MLS) on UARS, which measures upper tropospheric water vapor [Read *et al.*, 1995] but does not detect thin clouds.

2. The CLAES Instrument and Data

The instrument and operation have been described in detail by Roche *et al.* [1993]. In brief, CLAES acquired medium-resolution spectra of infrared thermal emission from the Earth's limb in nine channels ranging from 3.5 to 12.8 μm , corresponding to the altitude range of approximately 10–60 km. The viewing geometry of the 57° inclination UARS orbit provides for daily coverage extending from either 34°S to 80°N (north-look) or 34°N to 80°S (south-look), depending on the orientation of the spacecraft, which yaws 180° approximately every 36 days. With this coverage the tropics were continuously observed except for short calibration periods at the beginning and middle of the 36-day yaw period. A UARS measurement

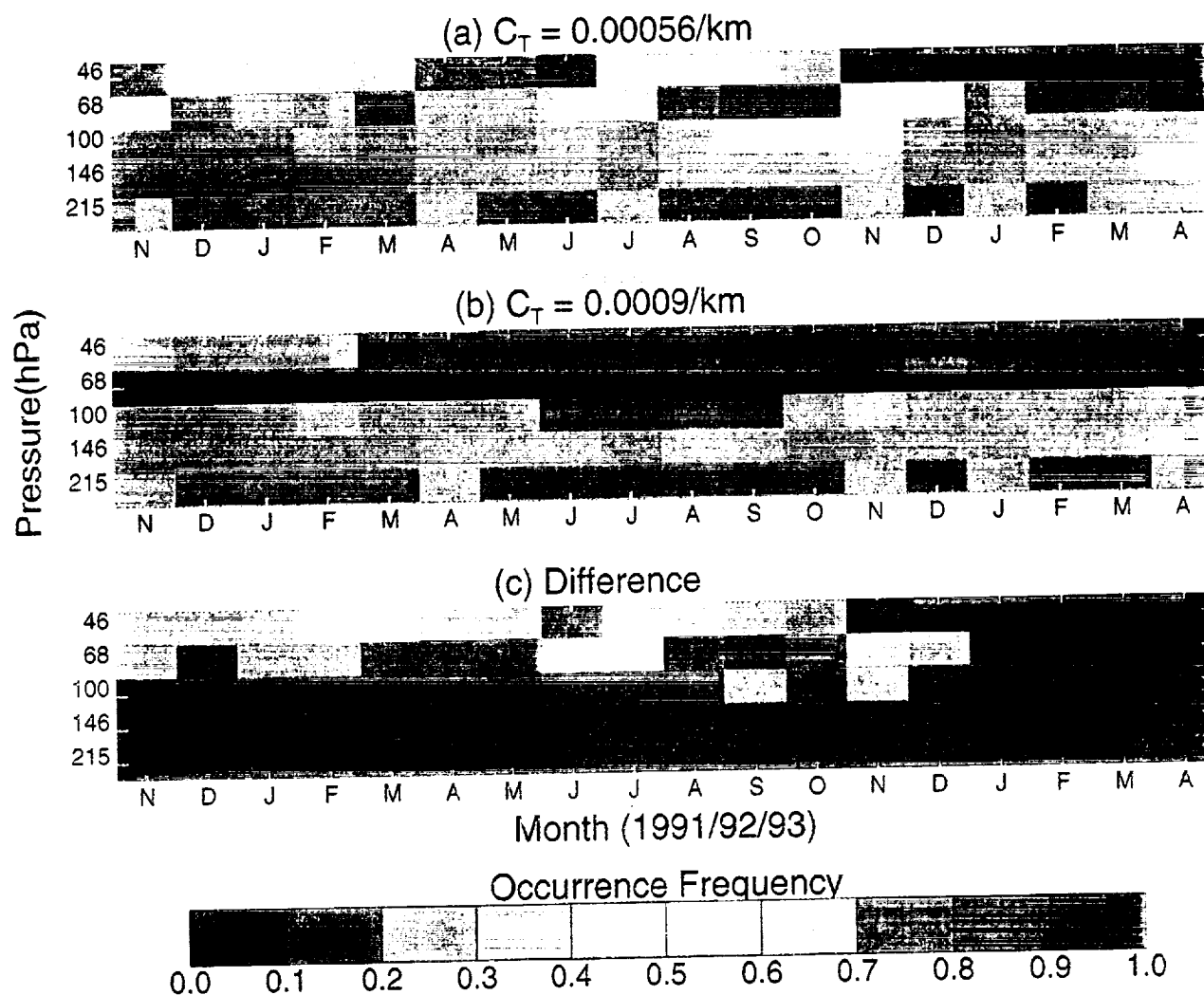


Plate 1. (a) The occurrence frequency of aerosol volume absorption coefficient $k_{\text{abs}}(12.8 \mu\text{m})$, in excess of the cloud identification threshold C_T for $C_T = 5.6 \times 10^{-4} \text{ km}^{-1}$. (b) A similar plot with C_T raised to $9.0 \times 10^{-4} \text{ km}^{-1}$ in which the Mount Pinatubo-related variation is no longer apparent in the 68- to 215-hPa layers. (c) The difference between Plates 1a and 1b shows the transient aerosol background rejected by increasing C_T .

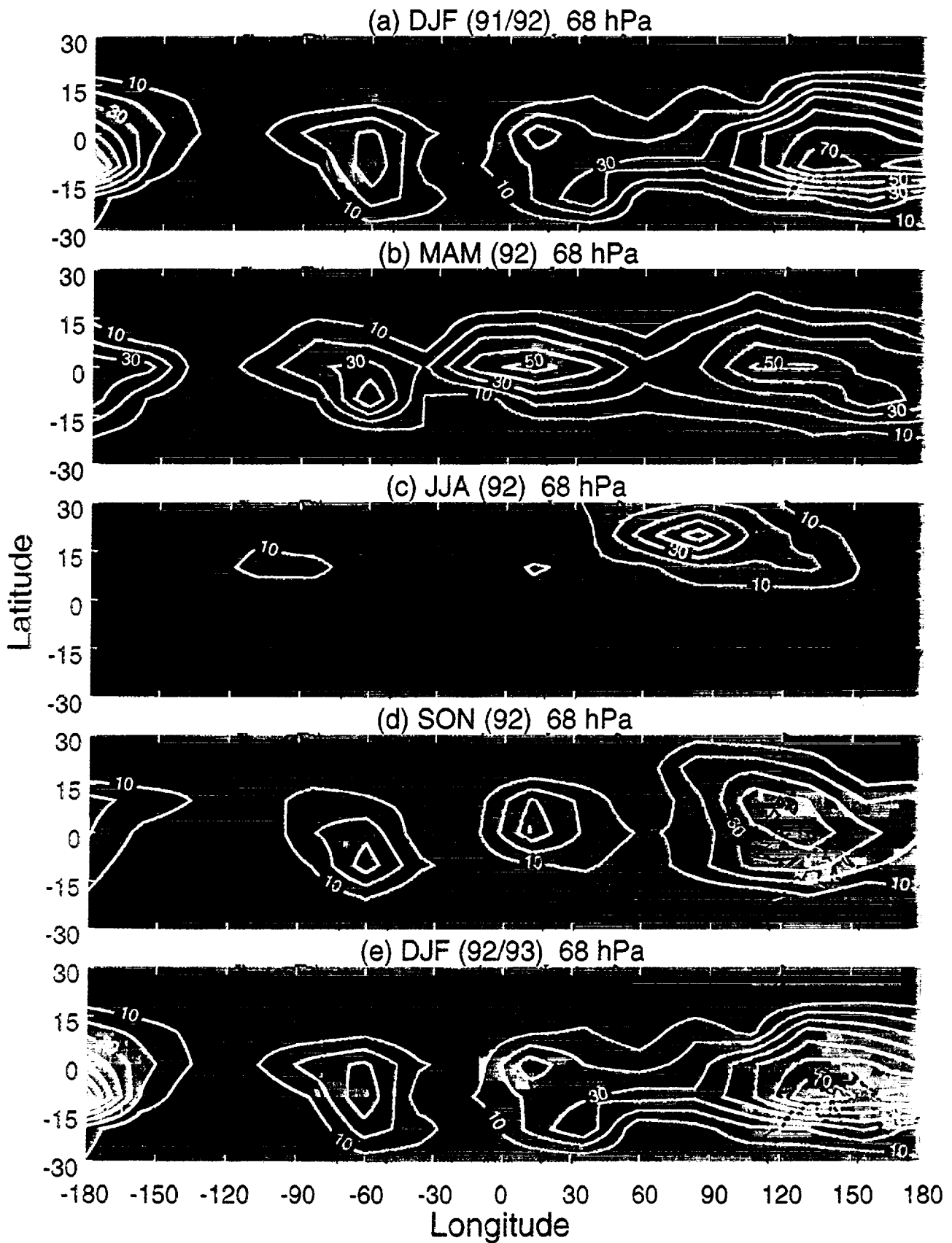


Plate 2. The seasonal cloud occurrence frequencies at 68 hPa derived from Cryogenic Limb Array Etalon Spectrometer (CLAES) (color) compared with the Stratospheric Aerosol and Gas Experiment (SAGE) II climatology [Wang *et al.*, 1996] (white overlay). (a) The CLAES observations for December, January, and February (DJF) of 1991–1992 overlain with climatology. The color scale is the same as Plate 1. (b) March, April, and May (MAM) 1992. (c) June, July, and August (JJA) 1992. (d) September, October, and November (SON) 1992. (e) December, January, and February (DJF) 1992–1993.

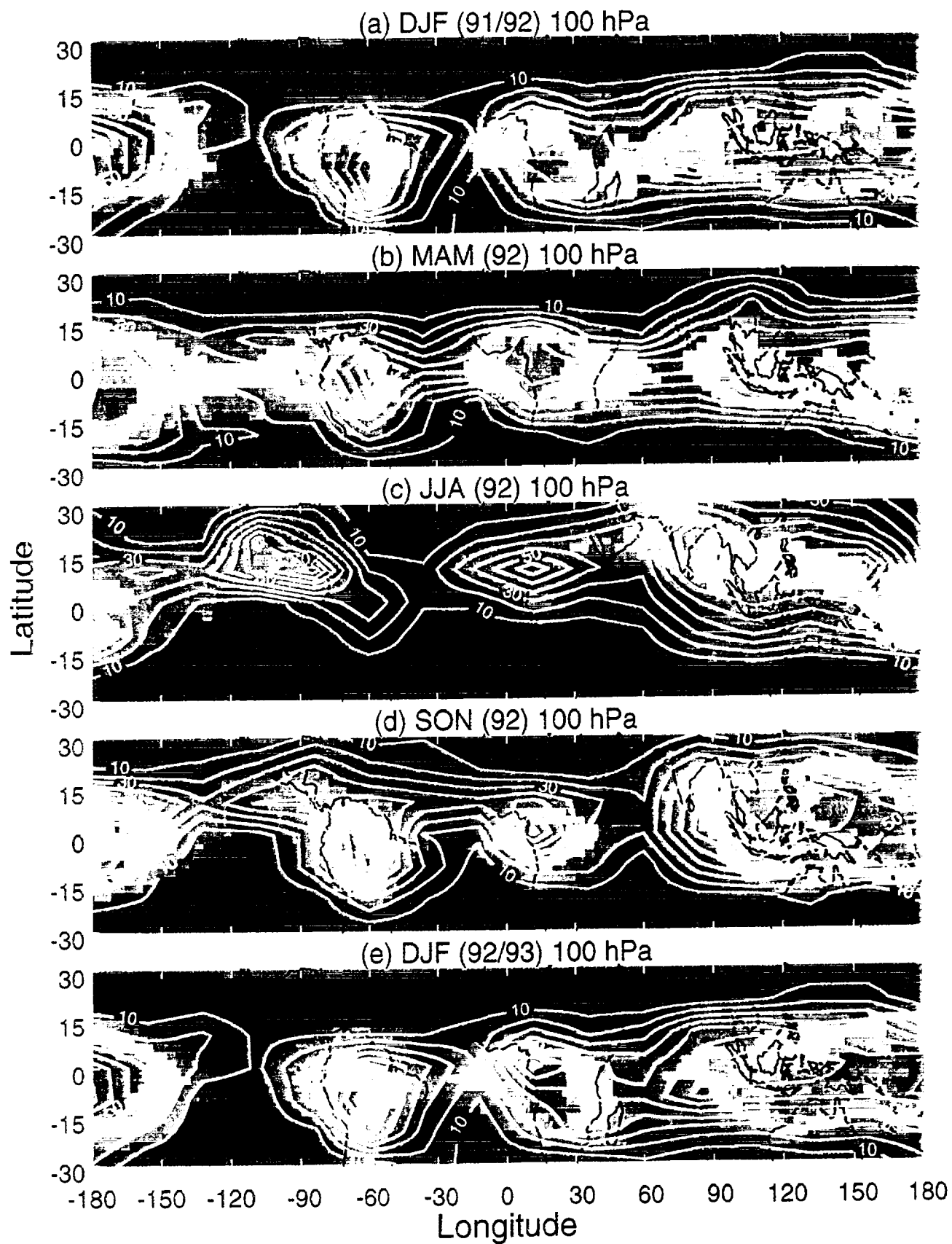


Plate 3. Same as Plate 2 except at 100 hPa.

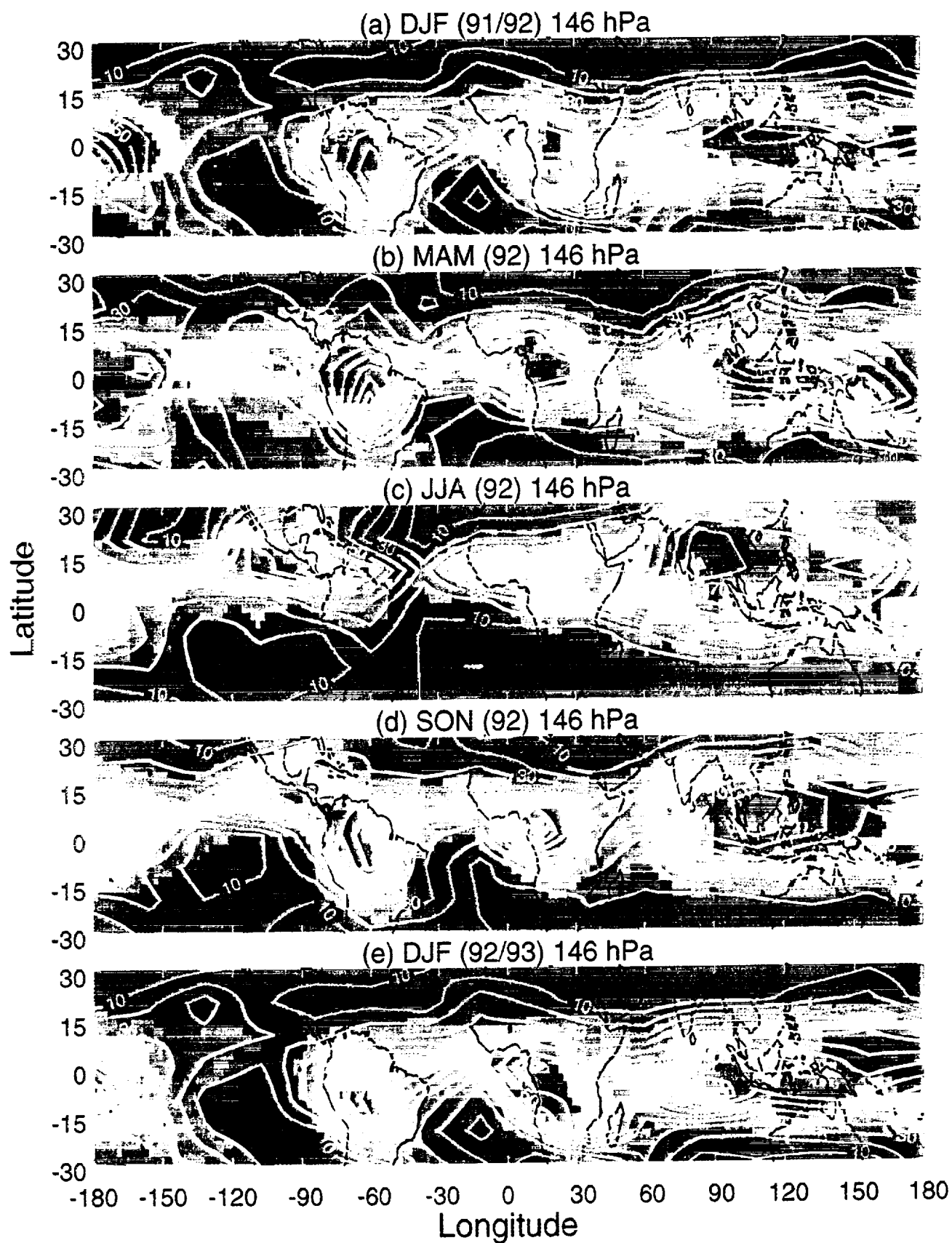


Plate 4. Same as Plate 2 except at 146 hPa.

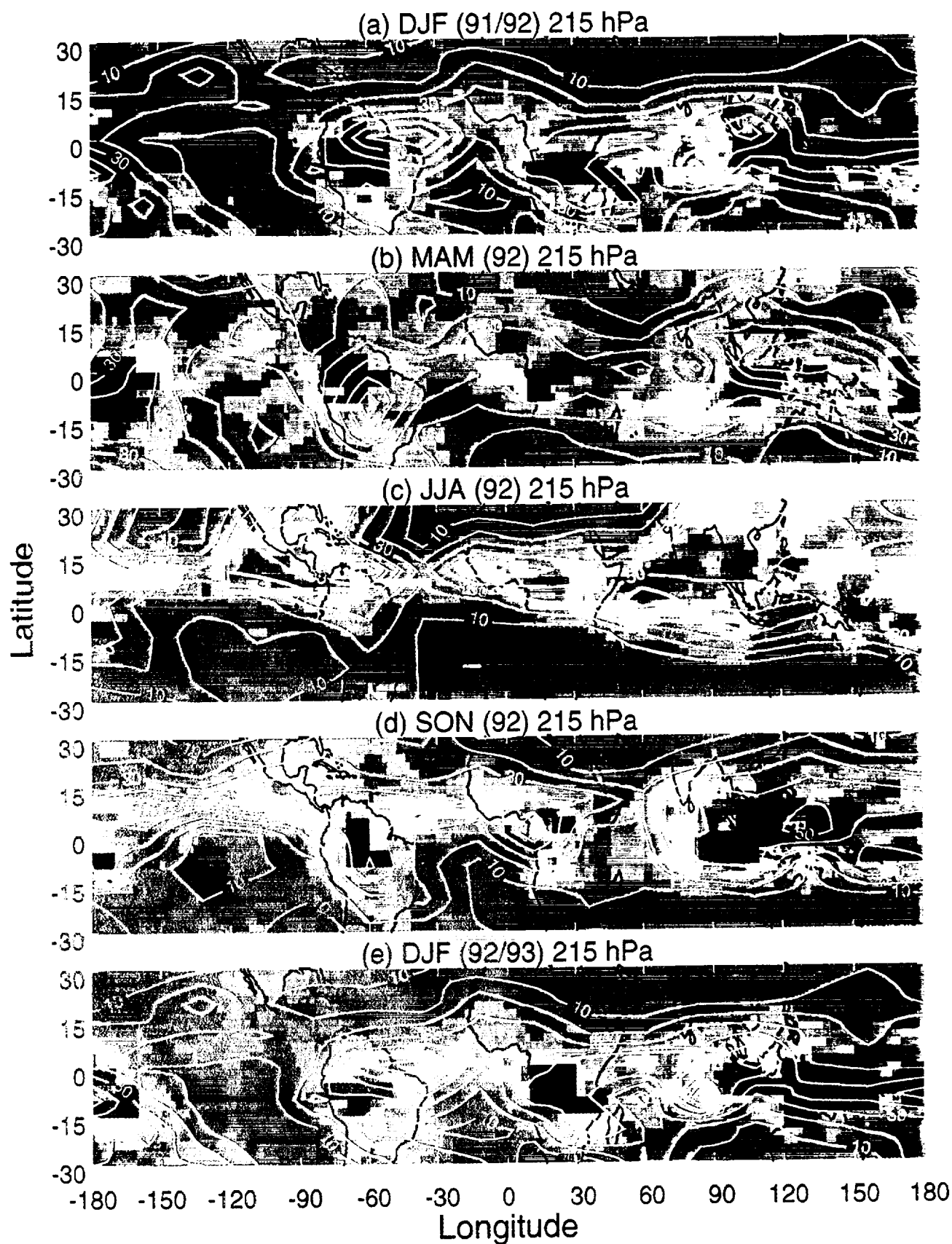


Plate 5. Same as Plate 2 except at 215 hPa.

bearing UARS pressure levels and consists of five panels, one for each season of CLAES observations. This analysis uses $C_T = 9.0 \times 10^{-4} \text{ km}^{-1}$ and $E_T = 30\%$ for the CLAES data. Sensitivity of the results to these parameters is discussed below. The color scale is the same as used in Plate 1. To make a CLAES versus SAGE II comparison without entirely reanalyzing SAGE II data to take into account differences in instrument vertical resolution, the Wang *et al.* [1996] statistics for various levels and cloud type have been combined to approximate CLAES results, which have a vertical resolution of 3.5 km on the UARS pressure levels. The SAGE II results are overlain in each panel in white contours.

Plate 2a shows cloud occurrence frequencies derived from CLAES measurements for the 68-hPa level from December 1991 through February 1992 (labeled DJF 91/92). Since the tropical 68-hPa surface is centered near 19 km, the CLAES measurements incorporate contributions down to about 17.0 km. This is a region of sharply declining cloud occurrence above the mean tropopause. The most comparable results from the Wang *et al.* [1996] climatology are the SVC data at 17.5 km. Notwithstanding magnitude differences, the spatial distribution of cloud occurrence frequency and its seasonal evolution agree quite well with the SAGE II results. Both data sets show similar patterns of cloud occurrence including maxima over Indonesia, equatorial Africa, the Amazon Basin, and the western Pacific. The March, April, and May (MAM) (Plate 2b) data from CLAES and SAGE II show qualitative spatial and temporal agreement. For example, both data sets reveal similar cloud occurrence frequency increases over equatorial Africa and reductions over the western Pacific and Indonesia.

In June, July, and August (JJA) (Plate 2c), both data sets show a minimum in tropical cloud occurrence and reasonably good agreement in spatial distribution. In the fall, September, October, and November (SON), both data sets show the progress of the annual cycle, with the return of higher cloud occurrences in the locations where high winter occurrences were noted.

An interesting aspect of the 68-hPa level is that this is a level where an interannual variation can be seen that can plausibly be linked to the Mount Pinatubo aerosol veil. This is shown by the increase in area exceeding the 10% frequency-of-occurrence level in DJF (1992–1993) (Plate 2e) relative to a year earlier. A possible explanation is that less convective activity reached this high level during DJF (1991–1992) due to the reduced penetration of solar radiation to the tropics. Another possible cause could be circulation changes associated with the 1991–1992 El Niño. It is hard to separate the influence of these two atmospheric perturbations based on the CLAES 19-month data set.

In general, the cloud occurrence frequency on this level (68 hPa) is less in the CLAES data than in the climatological data chosen for comparison. This occurs because the data sets compared are mismatched in altitude in the region of particularly sharp vertical gradients in cloud occurrence frequency. For instance, the center of the UARS 68-hPa level is in the lower stratosphere, but the CLAES effective field of view is wide enough to include the highest excursions of the tropopause. A better comparison might be attained by reanalyzing the SAGE II data on the UARS pressure grid at CLAES vertical resolution; however, data comparison could be difficult because the results are likely to be very sensitive to factors that contribute to the vertical resolution of the data set. Nevertheless, it is a

useful comparison because it shows the spatial distribution similarities in the data sets at the highest cloud-bearing levels.

Plate 3 shows the seasonal cloud occurrence frequency observations for the 100-hPa level. The tropical 100-hPa surface is centered near 16.5 km, and the CLAES measurements incorporate contributions from about 14.8 to 18.2 km. To avoid counting SAGE cloud occurrences more than once, the CLAES data are overlain with the climatological SAGE II 15.5-km SVC statistics only. Cloudiness at higher levels, notably 17.5 km, appears spatially well correlated with this level. The spatial distribution of CLAES and SAGE II observations agrees well for the 1991–1992 DJF season (Plate 3a) on the 100-hPa level. The geographical cloud distribution is also very similar in MAM (Plate 3b). A notable area of disagreement is the western Pacific, where the 1991–1992 CLAES data show higher cloud occurrence in the central Pacific. (This probable El Niño effect is discussed more below.) For the June–July–August (JJA) period (Plate 3c), both data sets agree very well, showing, for example, the shift in the maximum from the Amazon Basin to the west coast of Mexico. For the September–October–November (SON) period, the Northern Hemisphere (NH) fall (Plate 3d), both data sets show that strong maxima are reestablished over South America and equatorial Africa. Regions of minimal cloudiness are also in substantial agreement. The similarity of the CLAES observations of DJF 1991–1992 (Plate 3a) and DJF 1992–1993 (Plate 3e) provide evidence that Mount Pinatubo aerosol has been rejected.

In all seasons the CLAES data appear to be more spatially confined than the SAGE II observations. This may be due to the relatively large bins used to accumulate SAGE II statistics or it may be due to higher SAGE II sensitivity at the edges of the cloudy regions. Otherwise, the SAGE II and CLAES observations at this level are in good agreement with respect to spatial distribution.

The good agreement between the CLAES cloud occurrence frequencies and the climatological SVC data, which are mostly subvisible cirrus [Wang *et al.*, 1994], is compelling evidence that CLAES detects subvisual cirrus in addition to thicker clouds. Plate 4 shows the seasonal progression of cloud occurrence on the 146-hPa level centered near 14.5 km. Comparable climatological data have been approximated on a grid-point by grid-point basis as the maximum of either the sum of the 13.5-km SVCs and 14.5-km OPCs or the 15.5-km SVCs alone. There are regions such as the vicinity of the Southern Pacific Convergence Zone (SPCZ) ($\sim 135^\circ\text{E}$, 25°S) where the SVC occurrence at 13.5 km is relatively high compared with the 15.5-km level, so cloud occurrences at the lower level would dominate the CLAES observations. Near the equator and the Intertropical Convergence Zone (ITCZ) the SAGE II data show that the 15.5-km level dominates the cloud count. In the SAGE II analysis an OPC occurrence on the 14.5-km level is independent of SVC occurrence at the 13.5-km level, since an opaque cloud event at 14.5 km precludes an SVC event below it. We assume that an SVC at 15.5 km is highly correlated with lower level OPCs due to the similarities of their geographical distributions seen in SAGE II data. Hence if the SVC maximum is at 15.5 km instead of 13.5 km, no opaque clouds are considered. This approximation may undercount OPCs with no overlying SVC. Areas of less frequent cloud occurrence are also in close agreement, including the fairly sharp decline northward of about 20°N and minima in the southern equatorial Atlantic and Pacific. In contrast to the 100-hPa observations, the 146-hPa level shows branching of the SPCZ and

ITCZ in the western Pacific. A notable difference in the CLAES and SAGE II cloud data is that clouds appear more frequently in the western Pacific. This is the "warm pool" area of high sea surface temperatures (SSTs) and high interannual variability in cloud cover associated with the El Niño [Chen and Houze, 1997]. Warm equatorial water had shifted toward the central Pacific in the NH winter of 1991–1992, showing the development of the mature phase of El Niño [Kousky, 1993]. The CLAES cirrus patterns of DJF 1992–1993 (Plate 4e) agree better with the SAGE II climatology. However, CLAES still shows relatively more cloudiness in the western Pacific.

On the 215-hPa level (Plate 5) between about 11.25 and 13.75 km the CLAES cloud frequency data are compared with the maximum climatological occurrence of either 13.5-km SVCs or 12.5-km OPCs. This is the level most influenced by overlying cloud. Note that there are blacked-out areas near some convectively active areas where overlying clouds allow fewer than four observations for the season. There are also fewer total measurements because the 215-hPa level is near the low-altitude limit of CLAES observations and is not sampled as frequently as higher altitudes. Compared with higher levels, clouds appear at higher latitudes since the tropopause region is included in the 215-hPa level beyond the tropics. The spatial patterns of cloud occurrence are not as well aligned with the SAGE II climatology as on higher levels.

As a further comparison with the SAGE II data, an averaged seasonal cloud occurrence frequency for observations within 20° of the equator has been computed. Plate 6 shows the seasonal cloud occurrence statistics for the layers centered at 68, 100, and 146 hPa. The bold black lines show the CLAES cloud occurrence frequency for $C_T = 9.0 \times 10^{-4} \text{ km}^{-1}$ and $E_T = 30\%$.

The dash-dotted lines in Plate 6 are a sensitivity test for C_T and show the results of a 44% increase in C_T to $1.3 \times 10^{-3} \text{ km}^{-1}$. Only the upper levels, 68 and 100 hPa, are sensitive to these changes in C_T . The dashed lines show the results of increasing E_T from 30% to 50%; this change has little effect at any level. Greater increases in E_T would eventually increase the cloud occurrence at the lower levels since it tends to cause cloud-obscured levels to be counted as cloud observations.

Plate 6a compares CLAES and SAGE II tropical cloud occurrence frequencies. As was qualitatively apparent in Plate 2, the SAGE II 17-km data show nearly twice the occurrence frequency as CLAES 68-hPa data, with the exception of JJA, where there is good agreement. Again, this discrepancy probably arises from a mismatch of levels in this region of high vertical gradient in cloud occurrence frequency.

The comparison on the 100-hPa surface (Plate 6b) shows numerical agreement between the climatology and CLAES better than 33% for all seasons, with MAM and SON cloud occurrence probabilities agreeing to within about 6%. However, the relative seasonal behavior of the 100-hPa CLAES data appears more like the 17.5-km climatological data (Plate 6a), i.e., the cloud occurrence frequencies are maximum in DJF, with a sharp minimum in JJA. This may be linked to vertical resolution differences between CLAES and SAGE II.

At 146 hPa (Plate 6c), CLAES observations and the climatology show agreement to better than 16% in the magnitude of individual season cloud occurrence. The relative season-to-season changes are also in good agreement. The 215-hPa level was not included because significant portions of it are obscured by overlying cirrus in the cloudiest periods.

Table 1 further illustrates the processing that resulted in

CLAES cloud occurrences. It is intended to give the reader a better understanding of the cloud-counting algorithm by summarizing the CLAES seasonal observational statistic for the region 20°S–20°N. For example, 22,705 (N_{total}) profiles were considered for DJF (1991–1992). Of these, 1848 (N_{cloud}) had a 68-hPa $k_{\text{abs}}(12.8 \mu\text{m})$ exceeding C_T , and of these profiles, 183 ($N_{E \leq 30\%}$) had error bars less than 30%. Of the measurements with low error, the average absorption coefficient was $1.10 \times 10^{-3} \text{ km}^{-1}$ ($k_E \leq 30\%$). N_{total} of 21,038 measurements at 100 hPa for DJF (1991–1992) are less than at the 68-hPa level because (1) most of the 68 hPa with $k_{\text{abs}}(12.8 \mu\text{m}) \geq C_T$ have been rejected from consideration because of large error bars and (2) owing to instrument pointing some profiles do not extend down to this level. Among the analysis characteristics illustrated by Table 1 are (1) the high number of measurements per season, (2) a measurement of $k_{\text{abs}} \geq C_T$ frequently results in the measurement being discarded at lower levels, and (3) at lower levels few measurements have error bars less than E_T .

5. Discussion and Conclusions

The empirical threshold method devised to identify clouds in the CLAES aerosol data appears to produce results that are in substantial agreement with the Wang *et al.* [1996] cloud climatology derived from SAGE II measurements. However, several factors both instrumental and atmospheric could influence the comparison of CLAES and SAGE II climatological cirrus data. Perhaps the most obvious instrumental differences between SAGE II and CLAES are sensitivity differences associated with the wavelengths of radiation used to probe the atmosphere. Differences in sampling volume can also influence the counting of cloud occurrences. Finally, the atmospheric state varies from year to year.

Wavelength-related cloud-counting differences between the SAGE II and this analysis of CLAES data were examined by relating the published thresholds for cloud detection for the SAGE II climatology with C_T using theoretical computations. For instance, the SAGE II climatology includes clouds with $k_{\text{ext}}(1.02 \mu\text{m}) \geq 2 \times 10^{-4} \text{ km}^{-1}$. For CLAES measurements, C_T has been set so that only occurrences of $k_{\text{abs}}(12.8 \mu\text{m}) \geq 9 \times 10^{-4} \text{ km}^{-1}$ are counted as clouds. To relate these thresholds, a Mie code was used to calculate extinction $k_{\text{abs}}(12.8 \mu\text{m})$ and absorption coefficients $k_{\text{ext}}(1.02 \mu\text{m})$ (see Table 2) for various hypothetical cloud particle size distributions. The calculations were based on a lognormal size distribution with width $\sigma = 1.7$ and ice optical properties of Warren [1984]. To examine particle size dependence, the mode radius of the size distribution was adjusted until the computed effective radius R_{eff} [Hansen and Travis, 1974] was one of the values in Table 2, left column. A factor was computed to normalize the particle distribution such that $k_{\text{abs}}(12.8 \mu\text{m}) = C_T$. This factor was also used to normalize the ice water content (IWC) and $k_{\text{ext}}(1.02 \mu\text{m})$.

Analysis of Table 2 reveals some interesting results. First, the SAGE II cirrus classification scheme should include much thinner clouds. Depending on particle size, the $k_{\text{ext}}(1.02 \mu\text{m})$, corresponding to the C_T established for $k_{\text{abs}}(12.8 \mu\text{m})$ during this volcanically perturbed period, is 8–35 times larger than the lower limit of SAGE II cloud detectability used to construct the Wang *et al.* [1996] climatology. On average, this ratio is expected to be near the larger end of this range because the particles are believed to be small. For example, Wang *et al.*

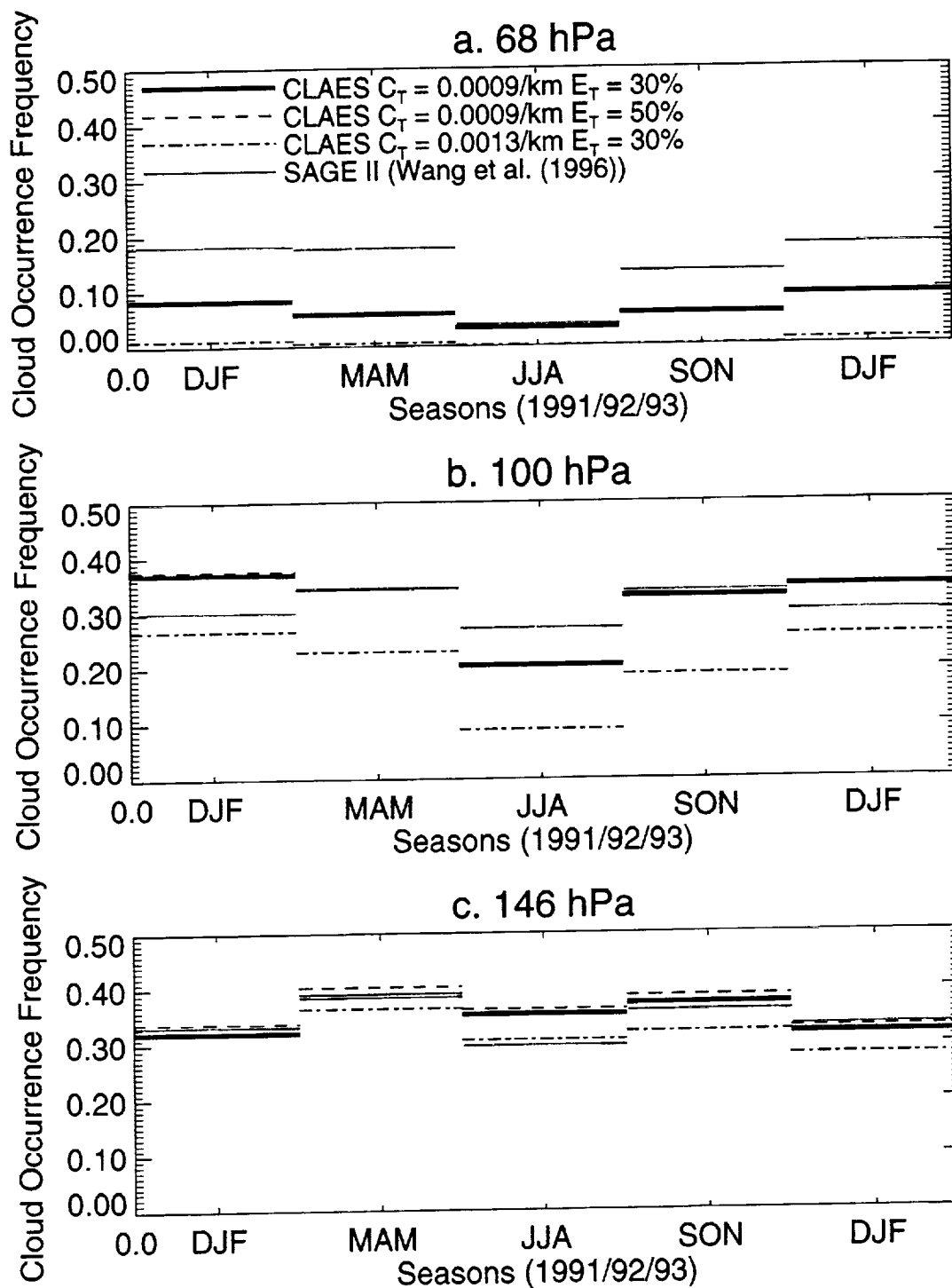


Plate 6. Multilevel comparisons of CLAES average seasonal cloud occurrence statistics for observations within 20° of the equator with the Wang et al. [1996] SAGE II climatology (red line). The CLAES cloud occurrence frequency for $C_T = 9.0 \times 10^{-4} \text{ km}^{-1}$ and $E_T = 30\%$ is shown by bold lines. The sensitivity to C_T and E_T (see text for definitions) is explored by cases with $C_T = 9.0 \times 10^{-4} \text{ km}^{-1}$ and $E_T = 50\%$ (dashed lines) and $C_T = 1.3 \times 10^{-3} \text{ km}^{-1}$ and $E_T = 30\%$ (dash-dotted lines).

[1995b, p. 3181] conclude that "the effective radius of most, if not all, of the high altitude clouds, measured by the SAGE series of instruments must be less than about $0.8 \mu\text{m}$." The result of this analysis is that one can expect to see differences in cloud occurrence identification which may vary as a function of the cloud particle size. Also, Wang *et al.* [1996] note that almost 70% of the unsaturated extinction coefficients are less than 0.008 km^{-1} . Given this predominance of low extinction measurements, one would expect to detect less than half the cloud occurrences detected by SAGE II as SVCs. On the basis of particle size, observation wavelength, and cloud detection threshold, this analysis of CLAES data should detect a significantly lower frequency of cloud occurrence than the SAGE II climatology and the discrepancy should increase for smaller cloud particle size.

We considered that the interannual differences in the 68-hPa cloud occurrence frequencies may be due to aerosol-induced changes in cloud particle size as observed by Wang *et al.* [1995b] in the SAGE II data. They observed lower extinction in near-tropopause cirrus clouds in 1985, when the stratosphere was perturbed by the 1982 El Chichon eruption, than in subsequent years when the stratosphere was cleaner. They attributed this difference to a shift of the effective radius of cirrus particles from about $0.8 \mu\text{m}$ to smaller sizes. As shown in Table 2, $k_{\text{abs}}(12.8 \mu\text{m})$ is nearly insensitive to this size change for a given IWC, so a particle size shift without a change in IWC cannot explain the CLAES observations.

Another significant difference between CLAES and SAGE

Table 2. Mie Calculations Showing the Aerosol Extinction at the SAGE Observation Wavelength, $k_{\text{ext}}(1.02 \mu\text{m})$, and Cloud Ice Water Content That Correspond to the CLAES Cloud Threshold Value of $k_{\text{abs}}(12.8 \mu\text{m}) = 9.0 \times 10^4 \text{ km}^{-1} = C_T$ for Various Particle Effective Radii, R_{eff}

Effective Radius $R_{\text{eff}}, \mu\text{m}$	λ -SAGE II $k_{\text{ext}}(1.02 \mu\text{m}), \text{km}^{-1}$	Ice Water Content, $\mu\text{g m}^{-3}$
0.4	5.62×10^{-3}	2.85
0.6	6.45×10^{-3}	2.83
0.8	6.28×10^{-3}	2.84
1.0	5.76×10^{-3}	2.89
2.0	3.37×10^{-3}	3.38
4.0	1.97×10^{-3}	4.60
10.1	1.48×10^{-3}	9.30
20.2	1.52×10^{-3}	19.5

II is the sampling volume of the measurements. The SAGE II measurement is representative of a tangent point volume of about 200 km along the line of sight, 1.0 km high, 2.5 km wide, and 200 km long, while the "L3AT" CLAES data are representative of a volume ~ 3.5 km high, 60 km wide, and 400 km long. Thus the CLAES sampling volume is approximately 170 times as large. Depending on the spatial distribution of clouds, this sample volume difference may make a difference in counting cloud occurrence. Suppose that detectable cloudiness is fairly uniform over large areas so that the smaller sampling volume of SAGE II does not see between the clouds. Then SAGE II and CLAES should count a similar frequency of cloud occurrence. If cloudiness is patchy, then SAGE II would detect clear sky relatively more frequently than CLAES. With the prevalence of extended high-altitude laminar cirrus observed by the Lidar In Space Technology Experiment (LITE) [Winker and Trepte, 1998], it is not clear that cloud patchiness would contribute greatly to differences between CLAES and SAGE observations of cloud occurrence frequency, but this is a subject for further consideration in future work.

Another factor that could influence cloud detectability is scattering. The redirection of upwelling thermal radiation into the CLAES line of sight could significantly enhance the CLAES ability to detect thin cirrus. A simple calculation was performed to model this effect using Mie theory to estimate the scattering and absorption of particulates and FASCOD3 (Fast Atmospheric Signature Code, version 3) [Clough *et al.*, 1989] to compute the upwelling average intensity of radiation at $12.8 \mu\text{m}$. For example, the radiance emanating toward CLAES from a $0.8\text{-}\mu\text{m}$ -radius ice particle near the tropical tropopause over a 300-K surface, like the tropical ocean, could be enhanced by 25% by scattering compared with thermal emission alone. If the particles are larger, the enhancement increases. Since this emission would be interpreted as thermal emission, it artificially raises the retrieved $k_{\text{abs}}(12.8 \mu\text{m})$; this may be a factor putting more observations over the cloud detection threshold.

In addition to instrumental differences, there are also likely to be atmospheric differences between the climatology period and the CLAES observation period. The presence of heavy volcanic aerosol loading during the CLAES period has been mentioned. There are obvious differences in cloud positions associated with El Niño events in both the climatology period and the period of CLAES observations.

In summary, the major finding of this work is the good general agreement of seasonal cirrus occurrence frequencies

Table 1. CLAES Seasonal Observational Statistics for the Region 20°S – 20°N

	68 hPa	100 hPa	146 hPa	215 hPa
<i>December 1991 to February 1992</i>				
N_{total}	22,705	21,038	12,472	5,985
N_{cloud}	1,848	7,726	4,023	978
$N_{E \leq 30\%}$	183	747	461	144
$k_{E \leq 30\%}$	1.10	1.64	1.74	1.56
<i>March–April–May 1992</i>				
N_{total}	27,101	25,775	15,778	6,290
N_{cloud}	1,586	8,916	6,150	1,395
$N_{E \leq 30\%}$	262	964	795	173
$k_{E \leq 30\%}$	1.09	1.64	1.91	1.74
<i>June–July–August 1992</i>				
N_{total}	24,658	24,325	18,315	7,295
N_{cloud}	824	4,995	6,496	1,772
$N_{E \leq 30\%}$	495	1,085	1,065	342
$k_{E \leq 30\%}$	0.98	1.47	1.80	1.87
<i>September–October–November 1992</i>				
N_{total}	27,762	26,770	17,481	6,800
N_{cloud}	1,667	8,818	6,531	1,566
$N_{E \leq 30\%}$	676	2,466	1,620	372
$k_{E \leq 30\%}$	1.04	1.57	1.96	1.93
<i>December 1992 to February 1993</i>				
N_{total}	25,353	23,723	15,085	7,457
N_{cloud}	2,289	8,200	4,814	1,476
$N_{E \leq 30\%}$	663	1,834	1,068	223
$k_{E \leq 30\%}$	1.15	1.75	2.15	1.91

N_{total} is the total of CLAES observations of $k_{\text{abs}}(12.8 \mu\text{m})$ for a given season at a given level discounted by the layers obscured by overlying clouds, as discussed in the text. N_{cloud} is the number of observations contributing to N_{total} that are over C_T . $N_{E \leq 30\%}$ is the number of observations contributing to N_{cloud} with error bars less than 30%. and $k_{E \leq 30\%} \times 10^{-3} \text{ km}^{-1}$ is the average volume absorption coefficient for observations with error bars less than 30%.

DRAFT

1

Observations of Near-Tropopause Tropical Cirrus: A case study combining UARS and TOGA COARE data

J. L. Mergenthaler, E.S Claffin, A. E. Roche and J. B. Kumer

Lockheed Martin Advanced Technology Center, Palo Alto, CA

J. D. Spinhirne

NASA Goddard Space Flight Center, Greenbelt, MD

S. T. Massie

National Center for Atmospheric Research, Boulder, CO

Short title: OBSERVATIONS OF NEAR-TROPOPAUSE TROPICAL CIRRUS

Abstract.

Samples of cirrus observations by the cryogenic limb array etalon spectrometer (CLAES) are examined in the context of other measurements available during the intensive operations period (IOP) of the Tropical Ocean Global Atmosphere Coupled Ocean-Atmosphere Response Experiment (TOGA COARE). The combination of cloud data from the limb viewing CLAES and nearly coincident International Satellite Cloud Climatology Project (ISCCP) data developed from the geosynchronous meteorological satellite (GMS-4) is used to investigate the detection of near-tropopause cirrus. In particular, the limb viewing CLAES is a much more sensitive detector of very thin cirrus than the ISCCP DX analysis and is used to locate cirrus in the ISCCP imagery where no clouds are apparent.

The CLAES cloud top height measurements compare well with data from airborne visible and infrared lidar (VIRL) along an approximately 2500 km track. A comparison of cloud top heights derived from CLAES, VIRL and ISCCP DX analysis shows the ISCCP analysis tends to underestimate the cloud top height of cirrus particularly when the cirrus overlies other clouds. Multi-level cloud occurrence frequency (COF) statistics obtained from the CLAES data are used to plot the progress of two Madden Julian oscillation events during the TOGA COARE IOP.

Introduction

A complete description of the spatial and temporal distribution of cloudiness is essential to computing the earth's radiation budget and a first step to accurately predicting future changes. In addition to their radiative effects *Ramanathan and Collins* (1999), tropical clouds in the neighborhood of the tropopause are also of interest in studies of the hydration and dyhydration of the stratosphere [*Danielsen*, 1993; *Jensen et al.*, 1996 and *Sherwood and Dessler*, 1999] also contribute to heterogeneous chemical processes in the upper troposphere [*Solomon et al.*, 1997]. Considerable progress has been made in describing cloud properties from operational and experimental satellites. The vast majority of analysis has been applied to nadir viewing operational meteorological satellite data from instruments like the advanced very high-resolution radiometer (AVHRR) and the high-resolution infrared radiometer sounder (HIRS) on NOAA polar orbiting satellites or visible/IR radiometers on the geosynchronous orbiting environmental satellites (GOES) or Japan's geosynchronous meteorological satellite (GMS). Thin clouds with visible optical depths less than a few tenths are difficult to detect in nadir data, especially when they overlay lower level clouds or variable background or are so thin as to be considered subvisual i.e. optical depths less than about 0.04 [*Sassen and Cho*, 1992]. However, thin and subvisual cirrus cover vast areas of the tropics [*Prabakara et al.*, 1988], [*Wang et al.*, 1996] and [*Winker and Trepte*, 1998]. The most widely used data base describing the occurrence frequency and distribution of very thin or subvisual cirrus comes the Stratospheric Aerosol and Gas Experiment

(SAGE) II on the Earth Radiation Budget Experiment (ERBE) satellite [Wang *et al.*, 1996]. The SAGE system measures the intensity of solar beam through the earth's limb during sunrise and sunset [McCormick *et al.*, 1971]. This viewing geometry increases the pathlength through a 1 km thick atmospheric layer to over 200 km, thus gaining an enormous advantage in sensitivity over nadir sounders to the detection of thin clouds and aerosol.

The cryogenic limb array etalon spectrometer (CLAES) on the Upper Atmosphere Research Satellite (UARS) shares the limb geometry advantages of SAGE II for detecting very thin clouds and aerosol [Mergenthaler *et al.*, 1999], but unlike the solar occultation instrument which typically gathers fewer than four aerosol profile measurements per day in the tropics (20N to 20S), CLAES, which measures atmospheric infrared thermal emission, typically obtains 280 profiles. This work utilizes the higher data density of CLAES to examine limb observations on smaller time and spatial scales than practical with a solar occultation instrument. We compare these CLAES near-tropopause tropical cirrus observations with cloud-related data obtained during the Tropical Ocean Global Atmosphere Coupled Ocean-Atmosphere Response Experiment (TOGA COARE) intensive operations period (IOP).

The TOGA-COARE experiment from November 1, 1992 until March 1, 1993 was an endeavor to better understand the variability of the coupled ocean-atmosphere system in the Pacific "Warm Pool" region [Webster and Lukas, 1992]. As such, the experiment involved extensive aircraft, surface and satellite observations of the COARE region from 20°S to 20°N and from 130°E to 190°E with more intensive observation

concentrated in smaller domains in this area. One of the stated goals was to understand the processes that organize convection so cloud observations were a very important aspect of the experiment.

For the purpose of gaining insight and additional validation to the CLAES observations, we compare CLAES cirrus observations with more established cloud measurements from the NASA DC8-borne VIRT [Spinhirne, Hart and Hlavka, 1996] and cloud top height measurements from the International Satellite Cloud Climatology Project (ISCCP) [Rossow and Schiffer, 1991] developed from the GMS-4 data. Additionally, we present first-time limb-sounder-based multi-level near-tropopause (COF) observations of the near-tropopause cirrus associated with individual Madden Julian oscillations events, which organize the convection in this area on a 30-50 day scale [Chen and Yanai, 2000]. The CLAES unique perspective is used to show the distribution of cirrus including subvisual cirrus in relation to the outgoing longwave radiation measured by the GMS-4 and should be of use in assessing the development of thin cirrus in the neighborhood of the MJO and possible flight planning in future experiments.

CLAES Observations

CLAES, which operated from October, 1991 until May 1993, has been described in detail by Roche *et al.* [1993]. In brief, CLAES acquired medium resolution spectra of infrared thermal emission from the earth's limb in nine channels ranging from 3.5 to 12.8 μm and over an altitude range of approximately 10-60 km. The CLAES line-of-sight is

approximately perpendicular to the the tangent point track. The viewing geometry of the 57° inclination UARS orbit provides for daily coverage extending from either 34°S to 80°N, or 34°N to 80°S, depending on the orientation of the spacecraft which yaws 180° approximately every 36 days. With this coverage the tropics were continuously observed except for short calibration periods at the beginning and middle of the yaw period. A UARS measurement sequence is completed every 65.3 seconds or about every 500 km along the tangent point sampling path. During a complete measurement sequence each of nine filters relatively broad (Full Width Half Maximum (FWHM) = 10 cm^{-1}) is rotated into the optical. This isolates spectral features of one or more target species. The filters are used in conjunction with one of four higher resolution, FWHM = 0.3 cm^{-1} , etalons that are tilt tuned to sample several wavelengths selected to provide sufficient information content to separate contributions from target gases and aerosol in the isolated region. The general retrieval process, which infers vertical profiles of several gaseous species and aerosol volume absorption coefficient for each channel, is based on the development of *Rodgers et al.* [1976] and is described by *Kumer et al.* [1996].

This work uses “Level 3 Along Track” (L3AT) aerosol volume absorption coefficients that are interpolated to the time and position corresponding to the center of the the 65.3 s measurement and to the standard UARS pressure surfaces defined by $P \text{ (hPa)} = 10^{(3-N/6)}$ where N is the layer index. The layers centered at 215, 146, 100 and 68 hPa ($N = 4, 5, 6 \text{ \& } 7$) cover the region where tropical cirrus clouds are likely to be seen in CLAES data. As in our earlier work, *Mergenthaler et al.* (1999), the aerosol volume absorption coefficient, $k_{abs}(\lambda)$ retrieved from the long wavelength channel, $\lambda=12.8 \text{ }\mu\text{m}$

(780 cm^{-1}) has been used because of the relatively high contrast between H_2O clouds and sulfate aerosol.

The accuracy of cloud height determination is related, in part, to pointing accuracy. Detailed pointing validation using comparisons of retrieved products (e.g. temperature, ozone and Pinatubo aerosol volume absorption coefficient profiles) with other UARS instruments, ground and balloon experiments indicate that the line-of-sight was within 0.5 km of the correlative data [Roche, 2000]. With respect to cloud height determination specifically, we've compared the seasonal cloud frequency of occurrence frequencies for levels near and above the tropical tropopause from the SAGE II climatology [Wang *et al.*, 1996] and CLAES. The solid line in Figure 1 shows the seasonal cloud frequency of occurrence for the tropics (20S to 20 N) from CLAES at the 146, 100 and 68 hPa levels which are centered on average at about 18.6 16.5 and 14.2 km. The coarse dashed line shows SAGE II (subvisual) cloud frequency of occurrence at the 15.5 and 17.5 km levels from Wang *et al.* [1996]. The overall CLAES and SAGE II climatology COFs agree well although there are differences differences in cloud detection sensitivity and instrument field of view that have been discussed in [Mergenthaler *et al.*, 1999] One way of characterizing the difference is to represent the altitude difference between where CLAES and SAGE II measure equivalent cloud frequency of occurrence are by vertical lines which project to the linearly interpolated CLAES cloud frequency of occurrence from the SAGE values. The average altitude difference over all seasons is about 0.6 km and shows that on average an equivalent cloud frequency of occurrence is seen about 0.6 km higher in the CLAES data than the SAGE II climatology for these uppermost

cloud layers. This comparison provides some assurance that the COFS and cloud height determination from CLAES agree fairly well in an average sense with a more established source. CLAES height bias on the upper edge of the cloud distribution is at least partially due to the coarser vertical resolution of the CLAES "L3AT" data, 3.5 km, compared to 1 km for SAGE II.

TOGA COARE Observations

Visible ($0.6 \mu\text{m}$) and infrared ($11 \mu\text{m}$) images of the IOP area were acquired by the GMS-4. These data were used to produce ISCCP DX cloud products (3-hourly 30 KM sampled image pixels [*Rossow and Schiffer, 1999*]), including cloud type, cloud top temperature, cloud top pressure and others. Figure 2 shows cloud top temperatures from the ISCCP DX analysis for 12 UTC on January 19, 1993. The locations and times of the "L3AT" CLAES ascending node aerosol measurements have been superposed on the images. (Aerosol absorption coefficients are represented as aerosol limb emissivity i.e., $\epsilon_l = (1 - \exp(\int k_{abs}(12.8 \mu\text{m}) ds))$ where $k_{abs}(12.8 \mu\text{m})$ is the retrieved aerosol volume absorption coefficient measured the $12.8 \mu\text{m}$ channel and s is distance along the limb path. Here ϵ_l has been approximated by assuming a 400 km path of uniform aerosol.) The corresponding symbols have been filled with dots sized in proportion to the limb emissivity, ϵ_l , on the 100 hPa surface (A filled (white) symbol indicates opaque cloud, $\epsilon_l = 1$, and an open white circle indicates a relatively transparent limb, $\epsilon_l \simeq 0$). In addition, a sampling track (green line) from the NASA DC-8 visible and infrared cloud lidar (VIRL) [*Spinhirne et al., 1997*] is shown that has remarkable

spatial coincidence with a CLAES ground track on this day and makes for a convenient altitude registration check of CLAES data and comparison with ISCCP DX products. Red traces from selected points represent 6 hr back trajectories on the 375 K (100 hPa) potential temperature surfaces computed with the Goddard Automailer Trajectory Model (*Lait, Newman and Schoeberl*, private communication)

Figure 2 show that cirrus detected by CLAES are not always aligned with the cold tops of clouds seen in the ISCCP DX cloud top temperature data. To put the CLAES sensitivity to cirrus in perspective, the cloud detection threshold corresponds to an aerosol volume absorption coefficient of $9 \times 10^{-4}/\text{km}$ [*Mergenthaler et al.* 1999]. Threshold level clouds were distributed in a 2.5 km layer and would yield a vertical optical depth of 0.0023 and change the nadir scene for near-tropopause cirrus over a 300°K ocean by about $\Delta T = 0.16^\circ\text{K}$. In comparison, the ISCCP cloud detection limit over open ocean is $\Delta T = 3.5^\circ\text{K}$ (see Table 3.2.4 [*Rossow et al.*, 1996]). For example, clouds are detected near Yap and Guam (12.90-12.95 UTC) at more than 700 kilometers from the closest cold cloud tops recorded by ISCCP. There is nearly a one hour difference between the 12 UTC ISCCP analysis and the CLAES observation. There may have been cloud development in this area between the observations and we cannot rule out this possibility. *Liao, Rossow and Rind*, (1995) noted the ISCCP analysis was insensitive to 1/3 of the high altitude clouds detected by SAGE II. So it is not unexpected that we can find cases such as these.

Cloud Detection

The DC8 lidar, VIRL, sampling path shown in Figure 1 starts near Kapingamiringi (155°E, 12°N) at 6 UTC and ends near Townsville, Australia (147°E, 19°S) at 9 UTC on 01/19/93. Figure 3a shows a comparison of CLAES aerosol limb emissivity data taken between 11.15 and 11.24 UTC and the maximum cloud top heights recorded by VIRL several hours earlier. The lidar data are reported at 75 m vertical spacing and the sampling volume is very small compared to the limb-sounding CLAES that averages about 60 km along the tangent track, 400 km along the line of sight and about 2.5 km vertically for the L3AT data. Overall the result of this comparison is that CLAES data show agreement with the highest lidar cloud tops which vary from about 17 to 15 km along the flight track. Notably, both data sets show the cloud tops lowering on the approach to Townsville. That this is reasonably coincident comparison is further supported by 6 hour back trajectories extending from the CLAES measurements. The back trajectories show that the wind at cloud top height had not transported the parcels very far relative to the size of the CLAES sampling volume in 6 hours. Also

This exercise provides additional evidence that the vertical registration of the CLAES cirrus measurement is reliable within the resolution limitations of the CLAES vertical sampling.

While CLAES and the VIRL lidar show agreement with respect to cloud top height, the cloud top altitude along the DC8 flight derived from the ISCCP DX cloud top pressure (also shown in Fig. 3a) are usually much lower. To compensate for disparities

in observations times we've plotted the maximum cloud top height for a given image pixel from the 6, 9 or 12 UTC analysis. Figure 4 shows the DC8 altitude and the spatially smoothed 1064 nm cloud optical depth derived from VIRL. The VIRL optical depth was computed assuming a backscatter-to-extinction ratio of 25, suitable for cirrus. The optical depth data were smoothed over 300 profiles to facilitate visual comparison; this smoothing approximates resolution of about 0.33° along the longitude-projected flight track. The ISCCP 6 UTC products correspond closely to the beginning of the DC8 flight leg and the sun was still up, providing a visible channel for ISCCP analysis. The visible channel is important for the derivation for the heights of thin clouds and their optical depth [Rossow and Schiffer, 1991]. The point of the preceeding analysis is to suggest that (1) CLAES detects near tropopause clouds that agree well with nearly coincident lidar observations (2) that these high altitude clouds are not represented in the ISCCP analysis.

Cloud Development during TOAGA COARE

Figures 4, 5 and 6 show the equatorial cirrus occurrence frequency at 68, 100 and 146 hPa as a time series through the TOGA COARE Intensive Operations Period (IOP) from November 1, 1992 to March 1, 1993. The data was prepared by binning the "3AT" 780 cm^{-1} aerosol volume extinction data obtained within 5° of the equator in 10° longitude by 7 day bins. A cloud occurrence was counted by the criteria described in Mergenthaler *et al.* (1999) i.e. an extinction measurement at a given level was deemed a cloud detection if the volume extinction coefficient exceeded $9.0\text{E-}04$ /km and is not

obscured by overlying clouds. The cloud occurrence frequency (COF) for the 68 hPa level (Figure 4) is the uppermost UARS-grid level where tropical clouds are seen. Since the vertical resolution is about 3.5 km and this level is centered near 18.4 km it includes clouds above about 16.7 km. The outgoing longwave radiation (OLR) obtained from the NOAA Climate Diagnostics Center has overlaid (white contours) on figure 4. The OLR data has been averaged over 7 days and from 5°S to 5°N and over 10° longitude bins to match the CLAES COF data. The averaging raises the minimum OLR but still provides a method of tracking the convective activity associated with the MJO. This relative position of clouds seen by CLAES with the thick convective clouds that substantially reduce the OLR. Three familiar areas of deep convection are apparent on the OLR and CLAES COF data; these are the equatorial Africa (20° E), the Indian Ocean and maritime continent (60° E - 180° E) and the Amazon Basin (60°W). The dashed lines show the length of the IOP and the width of the COARE study region. The understanding MJO was one of the goals of TOGA COARE and so the events of this period have been studied extensively [e.g. *Yanai, Chen and Tung* (2000), *Chen and Yanai* (2000)] Two prominent Madden Julian Oscillation (MJO) events that occurred during the IOP are evident in the OLR contours. They begin in the Indian Ocean (60° E) in early December and January , respectively and propagate eastward reaching the dateline about a month later. Figure 4 shows that the clouds seen by CLAES and gridded to the UARS 68 hPa level are fairly well aligned the lowest OLR observed in the COARE area (dashed lines). The OLR and the CLAES COF data show the eastward propagation of both MJO events. CLAES shows cloudiness extending well beyond the

eastern border of the COARE region and beyond the low OLR region. This high cirrus is likely to be associated with the convection apparent in the low OLR data but we have not investigated the details of the connection. Figure 5 shows the CLAES COF data gridded on the 100 hPa surface. There is better agreement between OLR and CLAES COF. This level is centered nearly on the tropical tropopause and intersects more of the cloudiness that contributes to low OLR values. Again the CLAES COF show cloudiness well east of the date line. Figure 6 shows the CLAES COF data gridded on the 146 hPa surface. Blacked out area indicate regions where less than four measurements are available in a bin because clouds at upper levels obscure this level. While much of the low OLR area is blacked out, some regions such as from (80°E-120°E) in November through January where the low OLR values were evidently due to lower clouds.

Conclusions

The good agreement with VIRL along a 2500 km track provides assurance that CLAES maximum cloud top heights are reasonable.

We have used the CLAES data to examine the cloudiness associated with the MJO. This is the first time a limb sounder has been used to map the cloudiness associated with this very important intra-season event tropical troposphere. This global view of the MJO which includes even very thin near tropopause clouds should complement the extensive TOGA COARE data base by providing a thin cloud information not previous available. It should be useful in planning future experiments by showing the location of cirrus relative to convective centers.

This case study demonstrates some advantages of combining operational nadir soundings with information from the earthlimb emission instrument for detecting thin, upper level cirrus. The results are also applicable to the next generation of thermal emission limb sounding instruments like HRDRLS *Gille and Barnett, 1992* that is scheduled to fly on AQUA.

Acknowledgements

This work was performed under NASA contract NAS5-98044.

References

- In situ evidence of rapid, vertical, irreversible transport of lower tropospheric air into the lower tropical stratosphere by convective cloud turrets and by large-scale upwelling in tropical cyclones, *J. Geophys. Res.*, **98**, 8665-8692, 1993.
- Chen, B. and M. Yanai, Comparison of the Madden-Julian oscillation (MJO) during the TOGA COARE IOP with a 15-year climatology, *J. Geophys. Res.*, **105**, 2139-2149, 2000.
- Gille, J.C. and J. J. Barnett, The high resolution dynamics limb sounder (HIRDLS). An instrument for the study of global change, *Rend. Sc. Int. Fis. Enrico Fermi*, **CXV**, 433-450, 1992.
- Jensen, E. J., O. B. Toon, L. Pfister, and H. Selkirk, Dehydration of the upper troposphere and lower stratosphere by subvisual cirrus clouds near the tropical tropopause, *Geophys. Res. Lett.*, **23**, 825-828, 1996.
- Kumer, J. B., et al., Comparison of correlative data with nitric acid data version 7 from the cryogenic limb array etalon spectrometer (CLAES) instrument deployed on the NASA Upper Atmosphere Research Satellite, *J. Geophys. Res.*, **101**, 9621-9656, 1996.
- Liao, X., W. B. Rossow, and D. Rind, Comparison between SAGE II and ISCCP high-clouds 1. Global and Zonal mean cloud amounts, *Journ. Geophys. Res.*, **100**, 1121-1135, 1995.

- Mergenthaler, J.L. , A.E. Roche, J.B. Kumer and G.A. Ely, Cryogenic etalon array spectrometer observations of tropical cirrus, *J. Geophys. Res.*, 104, 22,183-22,194, 1999.
- Prabakara, C., R.S. Fraser, G. Dalu, Man-Li, C. Wu and R.J. Curran, Thin cirrus clouds: Seasonal distributions over the oceans deduced from NIMBUS-4 IRIS, *J. Appl. Meteorol.*, 27, 379-399, 1988.
- Roche, A. E., J. B. Kumer, J. L. Mergenthaler, G. A. Ely, W. G. Uplinger, J. F. Potter, T. C. James, and L. W. Sterritt, The cryogenic limb array etalon spectrometer (CLAES) on UARS: Experiment description and performance, *J. Geophys. Res.*, 98, 10,763-10,775, 1993.
- Rodgers, C., Retrieval of atmospheric temperature and composition from remote measurements of thermal radiation, *Rev. Geophys.*, 14, 609-624, 1976.
- Rossow, W.B., and R.A. Schiffer, ISCCP cloud data products, *Bull. Amer. Meteor. Soc.*, 72, 2-20, 1991.
- W.B. Rossow and R.A. Schiffer, Advances in Understanding Clouds for ISCCP, *Bull. Amer. Meteor. Soc.*, 80, 2261-2286, 1999
- Rossow, W. B., M. D. Roiter, and C. L. Brest, International Satellite Cloud Climatology Project (ISCCP) description of new cloud datasets. WMO/TD 737, World Climate Research Programme (ISC and WMO), 115 pp, 1996.
- Sherwood, S. C. and A. E. Dessler, On the control of stratospheric humidity, *Geophys. Res. Lett.*, 27, 2513-2516, 2000.

- Solomon, S., S. Borrmann, R. R. Garcia, R. Portmann, L. Thomason, L.R. Poole, D. Winker, and M. P. McCormick, Heterogeneous chlorine chemistry in the tropopause region, *J. Geophys. Res.*, *102*, 21,411-21,429, 1997.
- Spinhirne, J.D., W. D. Hart, and D. L. Hlavka, Cirrus infrared parameters and shortwave reflectance relations from observations. *J. Atmos. Sci.*, *53*, 1438-1458, 1996.
- Spinhirne, J.D., S. Chudamani, J. F. Cavanaugh and J. L. Bufton, Aerosol and cloud backscatter at 1.06, 1.54 and 0.53 μm by hard target calibrated airborne Nd:YAG/methane Raman lidar, *Appl. Opt.*, *36*, 3475-3490, 1997.
- Wang, P. H., P. Minnis, M. P. McCormick, G.S. Kent, and K.M. Skeens, A 6-year climatology of cloud occurrence frequency from Stratospheric Aerosol and Gas Experiment II observations (1985-1990), *J. Geophys. Res.*, *101*, 29,407-29,429, 1996.
- Webster, P. J. and R. Lukas, TOGA COARE: The TOGA coupled ocean-atmosphere response experiment, *Bull. Amer. Met. Soc.*, *73*, 1377-1416, 1992.
- Winker, D. M., and C. R. Trepte, Laminar cirrus observed near the tropical tropopause by LITE, *Geophys. Res. Lett.*, *25*, 3351-3354, 1998.

Lockheed-Martin ATC, Palo Alto, USA.

Received January 29, 2000; revised ?? ??, 2000; accepted ?? ??, 2000.

Figure Captions

Figure 1. Seasonal cloud frequency of occurrence frequencies for levels near and above the tropical tropopause from the SAGE II climatology [*Wang et al.*, 1996] and CLAES. The solid line shows the seasonal cloud frequency of occurrence for the tropics (20S to 20 N) from CLAES at the 146, 100 and 68 hPa levels which are centered on average at about 18.6 16.5 and 14.2 km. The coarse dashed line shows SAGE II (subvisual) cloud frequency of occurrence at the 15.5 and 17.5 km levels from Wang et al. [1996]

Figure 2. Cloud top temperatures from the ISCCP DX analysis for 12 UTC on January 19, 1993 and the locations and times of the CLAES ascending node aerosol retrievals. The circular symbols representing the locations of CLAES measurements have been filled in proportion to the limb emissivity (see text for definition.) The sampling track of the DC8-borne VIRL is shown in green. Red traces from selected points represent 6 hr back trajectories on the 375 K (100 hPa) potential temperature surfaces computed with the Goddard Automailer Trajectory Model.

Figure 3. (a.) The cloud top height (CTH) detected by three methods are shown. Cloud top location determined with the CLAES instrument is indicated by high emissivity in profiles (filled circles) acquired 11.15 and 11.24 UTC in the region of the DC8 flight track. (See Figure 2.). The VIRL cloud top heights (green dots) were recorded between 6 and 9 UTC when the lidar moved from 156 to 157°E then back to 147°E. The 6 UTC ISCCP DX cloud top height data (blue dashes) correspond in location to the lidar path. The DC8 altitude (dash dot line) is shown for reference. (b.) Cloud optical depths from VIRL. The total the above-the-aircraft integrated cloud optical depth (1064 nm) from VIRL (dashed line) corresponding to the cloud top heights above.

Figure 4. Figures 4. The equatorial cirrus occurrence frequency at 68 hPa as a time series through the TOGA COARE IOP from November 1, 1992 to March 1, 1993. The outgoing longwave radiation (OLR) obtained from the NOAA Climate Diagnostics Center has overlaid (white contours). The dashed lines show the length of the IOP and the width of the COARE study region

Figure 5. Same as Fig. 4 at 100 hPa.

Figure 6. Same as Fig. 5 at 146 hPa.

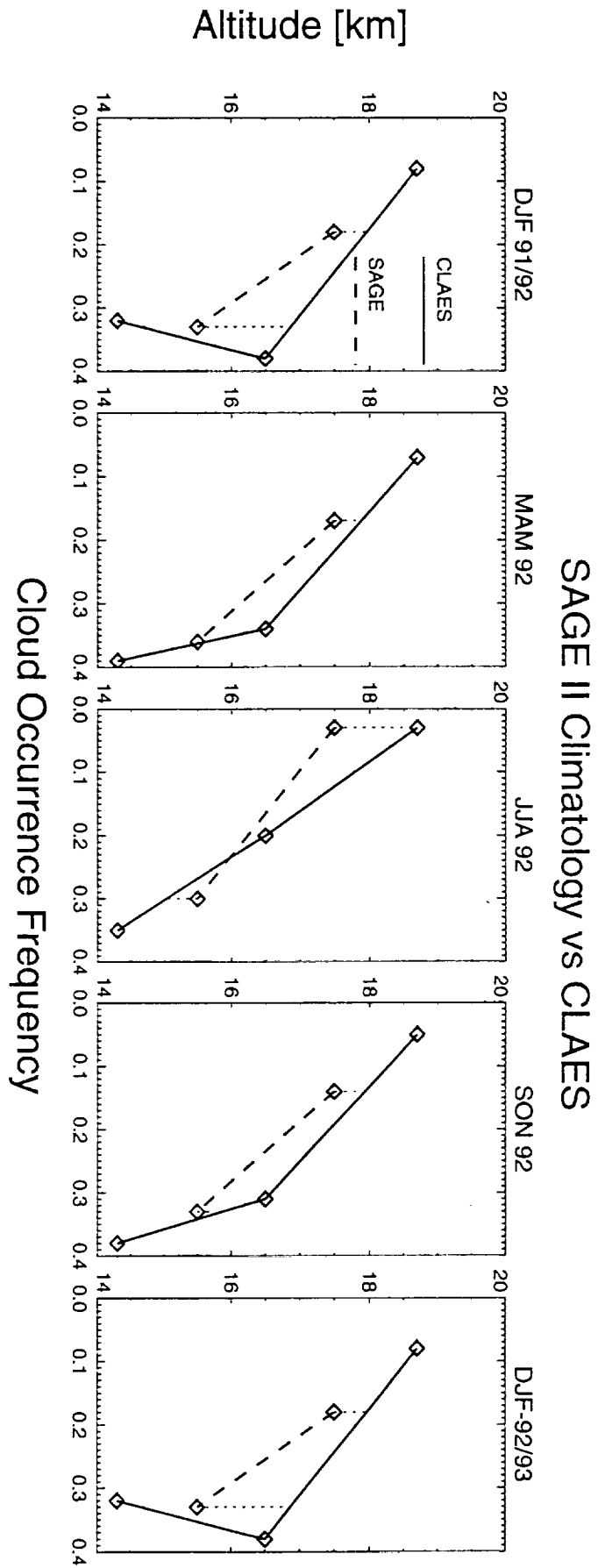


Figure 1

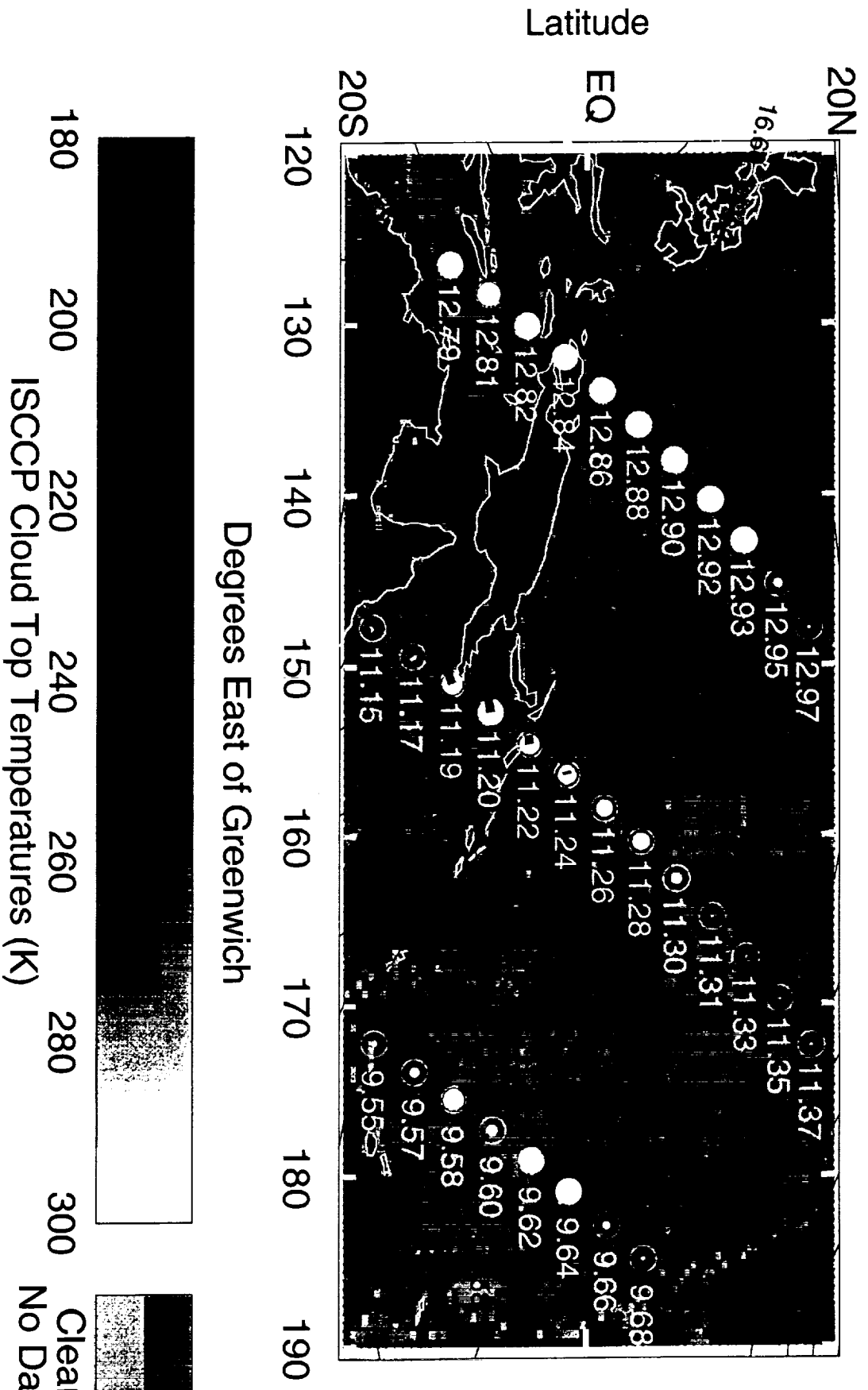


Figure 2

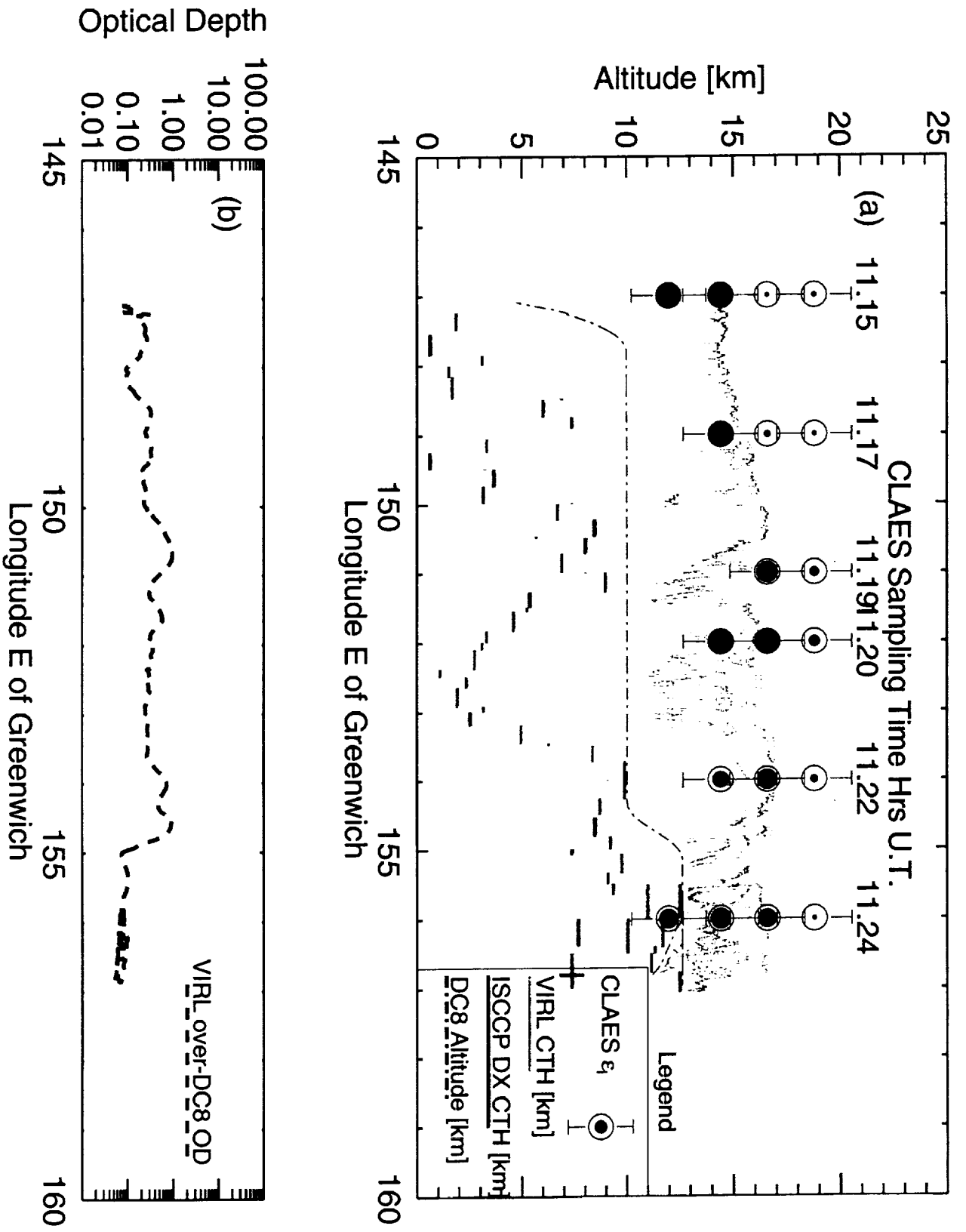


Figure 3

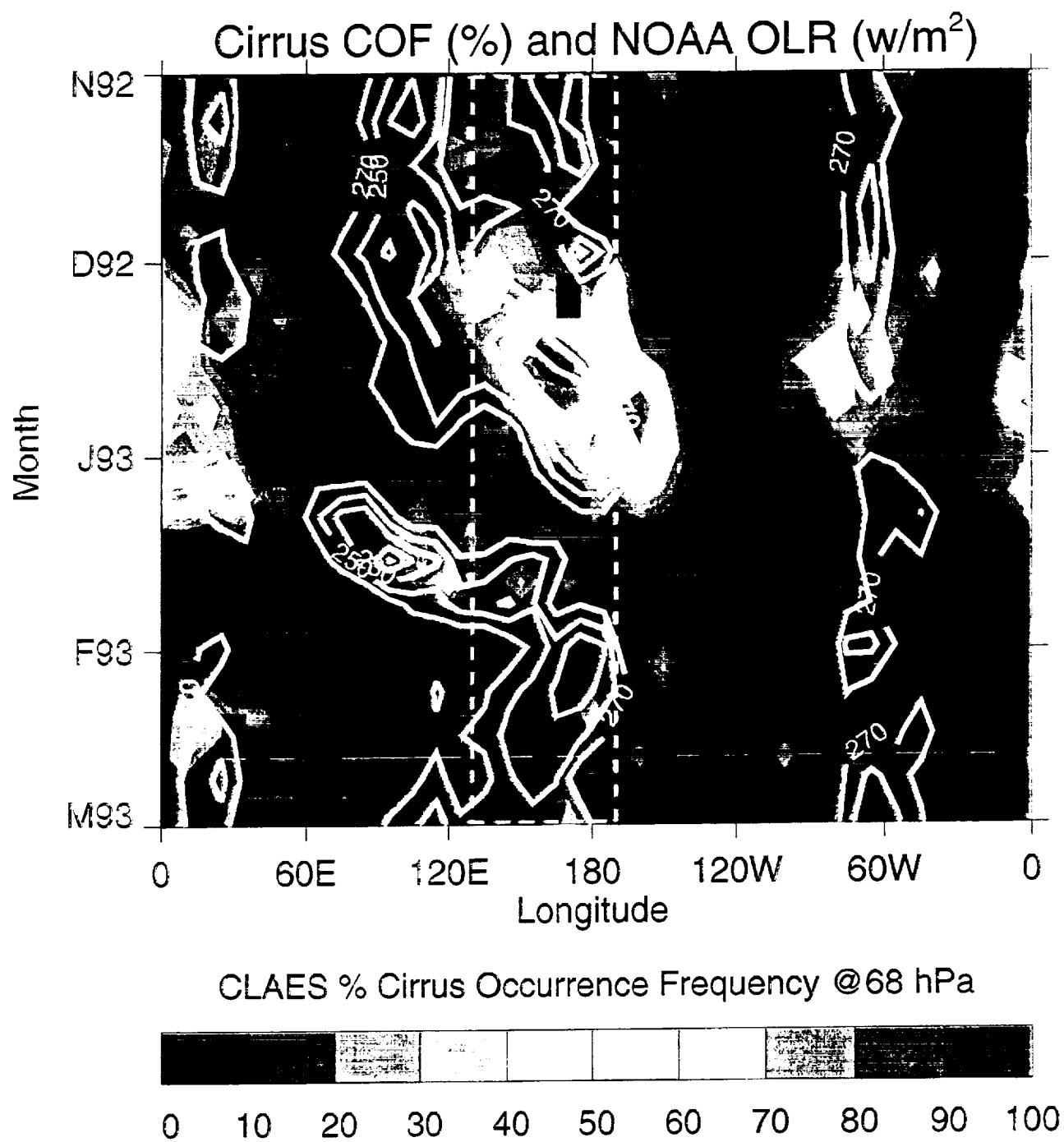


Figure 4

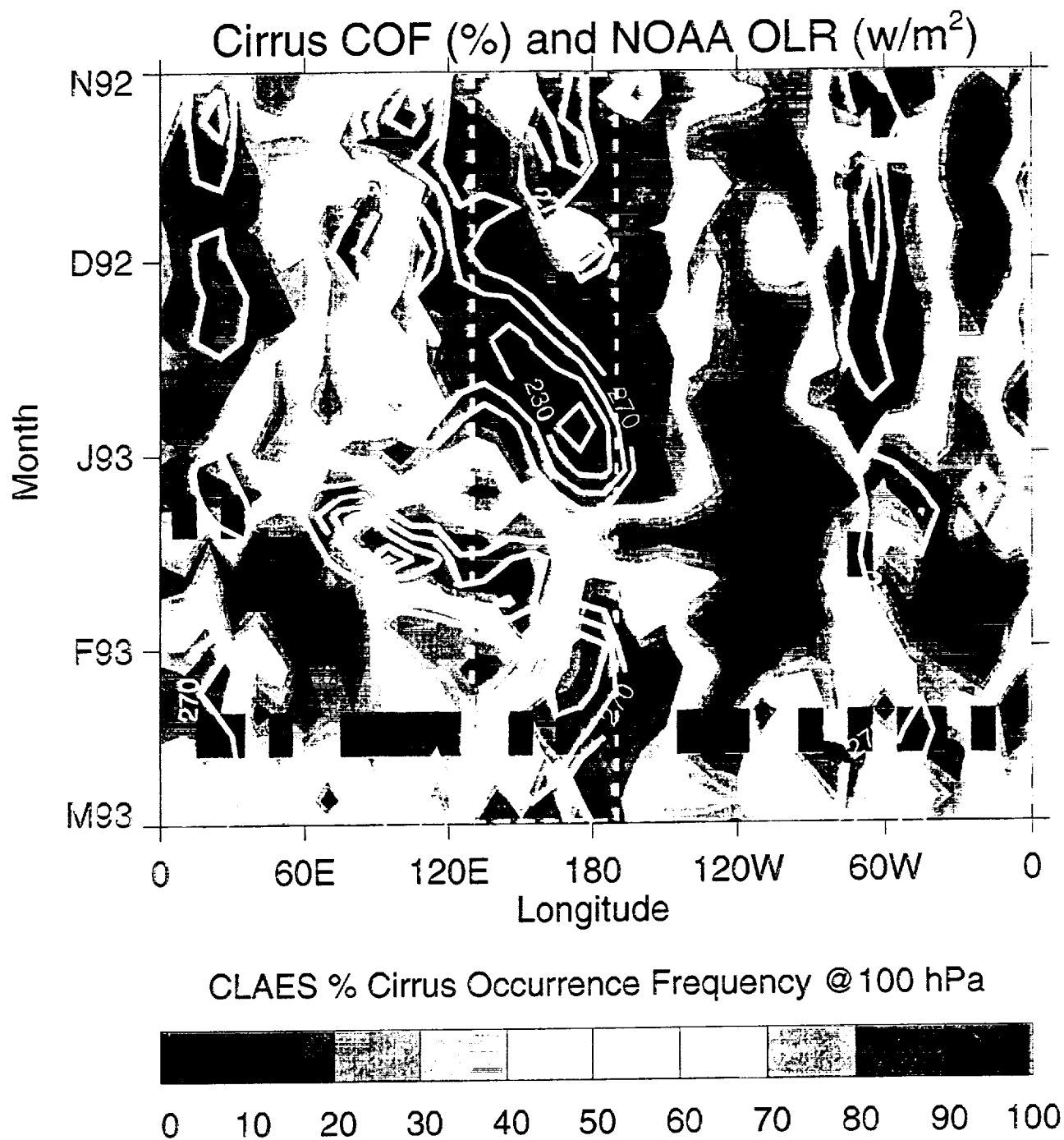


Figure 5

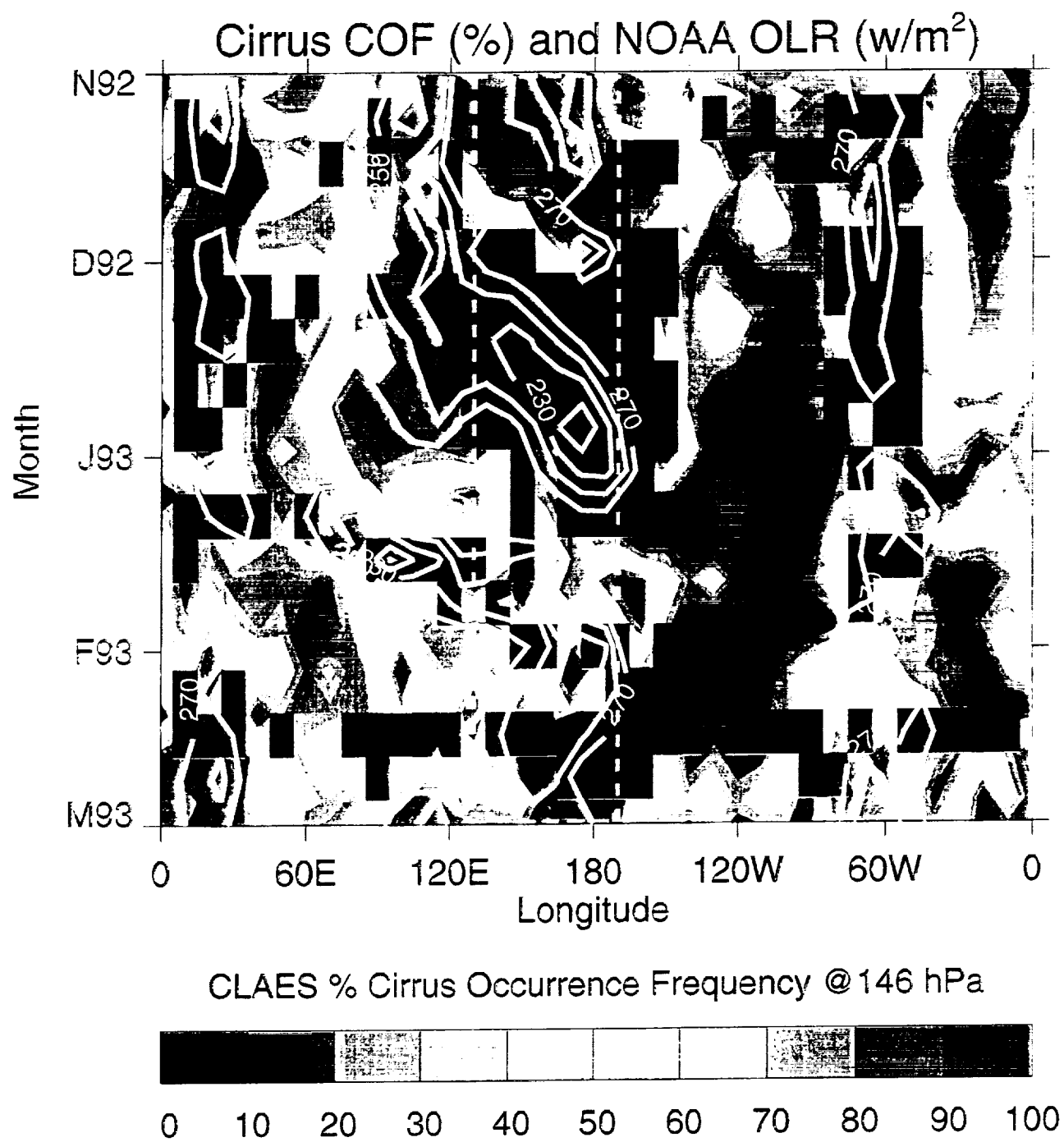


Figure 6